The FEBS Journal

FEBS PRESS science publishing by scientists

STATE-OF-THE-ART REVIEW

The more the merrier: effects of macromolecular crowding on the structure and dynamics of biological membranes

Maryna Löwe[1], Milara Kalacheva[2], Arnold J. Boersma[2] and Alexej Kedrov[1]

1 Synthetic Membrane Systems, Institute of Biochemistry, Heinrich Heine University Düsseldorf, Germany
2 DWI Leibniz Institute for Interactive Materials, Aachen, Germany

Keywords
anomalous diffusion; clustering; glycocalyx; intrinsically disordered proteins; membrane dynamics; membrane morphology; phase separation; protein:protein interactions; rafts; sensors

Correspondence
A. Kedrov, Heinrich Heine University Düsseldorf, Düsseldorf, Germany
Tel: 0049 211 81 13731
E-mail: Kedrov@hhu.de
and
A. J. Boersma, DWI Leibniz Institute for Interactive Materials, Aachen, Germany
Tel: 0049 241 80 23335
E-mail: Boersma@dwi.rwth-aachen.de

(Received 21 February 2020, revised 18 May 2020, accepted 19 May 2020)

doi:10.1111/febs.15429

Proteins are essential and abundant components of cellular membranes. Being densely packed within the limited surface area, proteins fulfil essential tasks for life, which include transport, signalling and maintenance of cellular homeostasis. The high protein density promotes nonspecific interactions, which affect the dynamics of the membrane-associated processes, but also contribute to higher levels of membrane organization. Here, we provide a comprehensive summary of the most recent findings of diverse effects resulting from high protein densities in both living membranes and reconstituted systems and display why the crowding phenomenon should be considered and assessed when studying cellular pathways. Biochemical, biophysical and computational studies reveal effects of crowding on the translational mobility of proteins and lipids, oligomerization and clustering of integral membrane proteins, and also folding and aggregation of proteins at the lipid membrane interface. The effects of crowding pervade to larger length scales, where interfacial and transmembrane crowding shapes the lipid membrane. Finally, we discuss the design and development of fluorescence-based sensors for macromolecular crowding and the perspectives to use those in application to cellular membranes and suggest some emerging topics in studying crowding at biological interfaces.

Introduction

Biological membranes are essential and intrinsically complex boundaries for individual cells and intracellular organelles. Amphipathic lipid molecules arranged into an anisotropic bilayer form the elementary membrane that is capable to prevent the passage of ions, polar solutes, and macromolecules, and to maintain the unique and specific lumenal contents (Fig. 1A). Next to this barrier function, cellular membranes serve as interfaces for biochemical reactions within vital cellular pathways, such as energy metabolism, signal transduction and transport processes, and the membrane organization largely determines the identity and functionality of the cells and their compartments [1,2]. The vast majority of functions are carried out by

Abbreviations
AFM, atomic force microscopy; AMPA, α-amino-3-hydroxy-5-methyl-4-isoxazolepropionic acid; BAM, β-barrel assembly machinery; BSA, bovine serum albumin; CCT, CTP-phosphocholine cytidylyltransferase; cryo-ET, cryo-electron tomography; ENTH, Epsin N-terminal homology domain; ER, endoplasmic reticulum; ESCRT, endosomal sorting complexes required for transport; FCS, fluorescence correlation spectroscopy; FP, fluorescent protein; FRET, Förster's resonance energy transfer; GFP, green fluorescent protein; GPCR, G protein-coupled receptor; GPMV, giant plasma membrane vesicle; GUV, giant unilamellar vesicle; IDR, intrinsically disordered region; IDP, intrinsically disordered protein; LD, lipid droplet; LHC, light-harvesting complex; LUV, large unilamellar vesicle; NMDA, N-Methyl-D-aspartate; OMP, outer membrane protein; PEG, polyethylene glycol; PSD, postsynaptic density; RBC, red blood cell; SPT, single-particle tracking; TMH, transmembrane helix; UPR, unfolded protein response.

integral proteins, whose hydrophobic domains are stabilized by interactions with apolar acyl chains of lipids, but also peripheral proteins that are adsorbed on the membrane via interactions with lipids or membrane-embedded proteins [3].

While the research on cytoplasmic proteins and their functional networks continuously flourished over the last half a century, the understanding of the membrane spatial organization lagged far behind. The early 'fluid mosaic model' of the membrane, which implied that proteins freely diffuse in the lateral directions within the fluid-like membrane, was based on the sparse data available on the membrane structure and dynamics (Fig. 1A) [4,5]. The model dominated the following decades, until technical developments in biophysical techniques, such as fluorescence, electron and atomic force microscopy, but also high-resolution proteomics and lipidomics, made it possible to visualize the actual complexity of the cellular membranes [6–12]. Today, cellular membranes are seen as heterogeneous mosaic environments, where structurally distinct domains with sizes ranging from tens of nanometers to micrometers serve as platforms for specific reactions, such as cell adhesion [13], chemoreception [14] or signalling [15].

The intrinsic complexity of cellular membranes

Both the phospholipid and the protein contents of cellular membranes are highly diverse and dynamic: in a single eukaryotic cell, hundreds of different lipid structures are unevenly distributed between organelles, and up to 25% of proteins synthesized in cells are inserted into membranes in a broad range of topologies [1,16]. The lipid composition greatly determines physicochemical properties of the membrane, such as fluidity, curvature and the asymmetric charge distribution. In the most general view, the endoplasmic reticulum (ER) membrane is relatively thin and loosely packed, while the plasma membrane is a rigid interface of a higher thickness, as determined by abundant sphingolipids and sterol molecules. Notably, the difference in the membrane composition between organelles is maintained despite the extensive vesicle trafficking, and the decisive sorting takes place within Golgi complex [2]. Fundamental roles of the lipids in the spatial organization of the membrane proteome have been revealed over the last two decades. Sphingolipids and sterol molecules abundant in the plasma membrane facilitate the separation of ordered and disordered phases at the

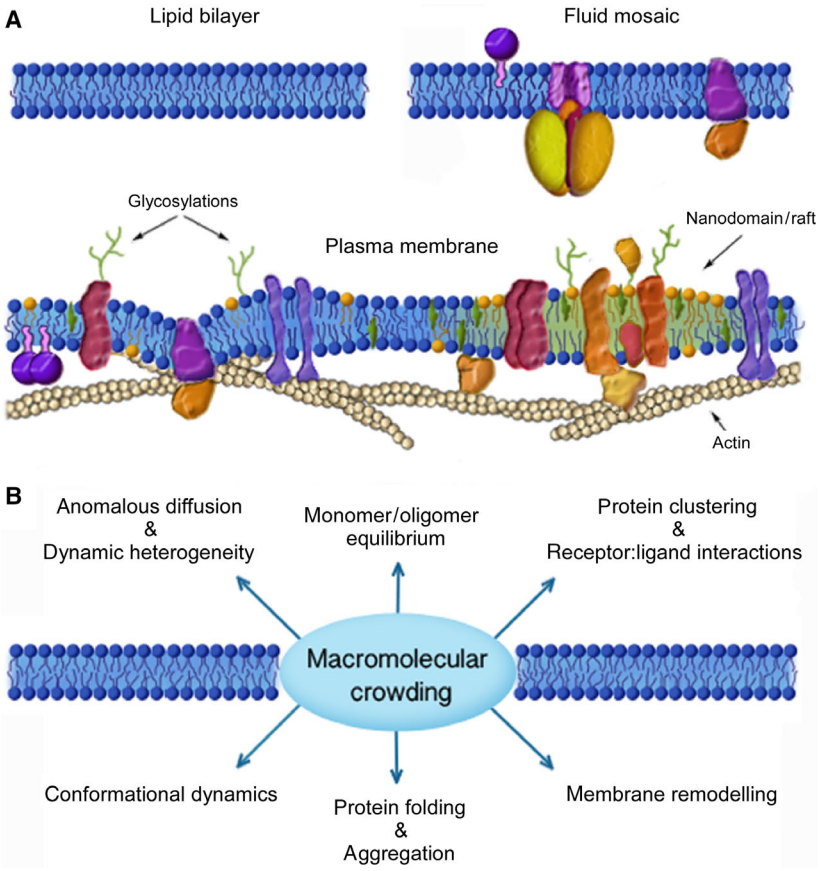

Fig. 1. Complexity of biological membranes. (A) Lipid bilayer (left) is an essential basis of a biological membrane. The membrane identity and functioning are determined by the composition of lipid molecules and proteins incorporated and anchored at the lipid bilayer. Low protein density is approximated by the 'fluid mosaic' model (right), while dense and specifically organized mosaic packing is commonly observed in membranes of living cells (bottom). Extensive interactions with the actin cytoskeleton affect the plasma membrane dynamics, and specific lipid: protein interactions build the ground for the assembly of densely packed membrane nanodomains, or rafts. (B) Macromolecular crowding affects a broad range of processes in biological membranes and contributes to the membrane morphology.

submicron scale and ensure the assembly of the functional raft domains with specific composition of densely packed proteins [6]. These domains are stabilized via protein:protein and protein:lipid interactions, as well as contacts with the cytoskeleton at the cytoplasmic side of the membrane (Fig. 1A), and their organization, dynamics and regulation have been recently reviewed elsewhere [15,17]. Furthermore, organelle-specific membrane thickness appears to determine the localization of integral membrane proteins along the trafficking pathway, so the optimal matching is achieved between the acyl chains and the hydrophobic transmembrane domains [18].

Membrane proteins constitute large part of cellular membranes and include not only integral proteins with transmembrane domains, but also soluble proteins peripherally bound to lipid leaflets via lipid anchors, hydrophobic interfaces or amphipathic helices, or docked on transmembrane proteins to form functional complexes [19,20]. The membrane proteome is highly dynamic, and substantial changes upon the development of pathologies, viral infections and between primary and immortalized cell cultures have been described [21–23]. Being abundant, membrane proteins may dominate the total membrane mass. Differences in membrane proteomes and protein abundance build a basis for the fractionation analysis of cellular organelles [24]. Literature provides several estimates for the area occupied by proteins in cellular membranes. In red blood cells (RBCs), one of the simplest mammalian cell types, transmembrane proteins such as the band 3 anion transporters and glycophorins occupy approximately 25% of the cellular membrane area, as suggested by the buoyant density and the dry mass measurements [25]. In a comprehensive analysis, the composition and the architecture of a synaptic vesicle from rat brain were described, offering an average protein:lipid mass ratio of 2 : 1 [26]. Data available on immortalized cell lines show a membrane protein occupancy around 40 000 to 50 000 per μm^2 in HeLa cells [21]. Alike, analysis of the protein synthesis rate and the density of the Golgi apparatus and ER membranes in hamster kidney cells provided estimates of around 30 000 to 40 000 individual membrane proteins per μm^2 [27].

It is important to emphasize the diversity of protein densities naturally occurring in different cell types and even on individual membranes within the single cell [22]. Specialized membranes or mesoscopic membrane domains commonly demonstrate higher protein densities, as those may be beneficial for assembly of functional complexes within the membrane and at the membrane interface. High protein density, 40 to 50% of the surface area, was reported for the inner mitochondrial membranes based on electrophoretic displacement experiments [28]. The density roughly corresponds to an average protein:lipid mass ratio of 4 : 1, with a substantial contribution of protein extramembrane domains, such as F_1 component of the ATP synthase. The density of rhodopsin packed in the specialized rod outer segment disc membranes is estimated to be 30 000 to 55 000 monomers per μm^2. This density corresponds to 50% of the surface area, using a monomer surface area of approximately 10 nm^2, in agreement with atomic force microscopy (AFM) imaging [29]. Probably, the highest degree of protein packing of ~ 80% is reached in plant thylakoid membranes and phototrophic microorganisms, where the high density of the light-harvesting complexes (LHCs) and reaction centres is vital for the efficient electron transfer within photosynthetic units [30,31].

Macromolecular crowding in solution and in the membranes

Macromolecular crowding has been commonly associated with the cytoplasm that contains a dense and highly diverse pool of macromolecules, the largest share of which are proteins and nucleic acids. The total concentration of macromolecules seen as crowding agents, or *crowders*, varies between 50 and 400 $g \cdot L^{-1}$, depending on cell type [32,33]. Both in solution and in the membrane, the crowders nonspecifically exclude volume from other cosolutes, providing an entropic penalty for larger cosolutes and reducing their configurational entropy [34]. The system attempts to reach a thermodynamic state of maximum entropy by providing more space to the crowders, which is commonly achieved by reducing the volume of another process. In addition to these sterics excluded volume effect, crowders present ample surface to interact promiscuously by noncovalent interactions. Hydrogen-bonding, hydrophobic, electrostatic and van der Waals interactions with other macromolecules, often referred as *soft* or *quinary interactions*, provide additional attractive and repulsive forces [35]. Different nature and shapes of crowders modulate the intermolecular interactions, but may also contribute to the change of the solvent properties, enhancing the effective intracellular viscosity and perturbed, or *anomalous*, diffusion [36,37]. Together, these contributions modulate translational mobility, conformational dynamics, assembly and functionality of macromolecules, determining the cellular organization and homeostasis. A multitude of effects of crowding on protein aggregation, folding, stability and oligomerization as well as catalytic

activity of enzymes and protein:protein interactions in solution has been documented and extensively reviewed elsewhere [34–36,38–40]. However, these effects, in particular the contribution of the quinary interactions, remain hard to predict because they depend on the size, shape, concentration of both the crowder and the biochemical reaction under investigation [36,41–43].

When the complexity and the patchwork-like organization of cellular membranes became evident, the significance of macromolecular crowding for the membrane-associated processes was rapidly anticipated, and the steadily accumulated data from multidisciplinary studies since reveal the diverse manifestations of crowding [44,45]. The consequences of macromolecular crowding in membranes and their interfaces may be more complex than observed in the solution due to the lipid membrane anisotropy and asymmetry observed in living cells [46]. Although smaller than proteins, lipids cannot be compared to water as a solvent and should also be seen as crowders, which extensively interact with embedded proteins via hydrophobic and electrostatic interactions. *Vice versa,* abundant proteins are changing the membrane structure within the hydrophobic core and at the polar interface, with a putative effect on the proximate aqueous solvent. Even at low protein:lipid ratios, the mobility of proteins within the lipid bilayer is limited to two-dimensional diffusion and it is largely determined by the bilayer viscosity [47]. Furthermore, lipid dimensions and physico-chemical properties may lead to sorting and clustering of membrane proteins in a concentration-dependent manner [18,48]. On the other hand, membrane proteins interfere with and restructure their proximal lipid environment, and protein crowding in lipid membranes may cause immense changes in the lipid packing and the membrane morphology. Finally, macromolecular crowding in the aqueous phase affects interactions at the membrane as well. It enhances protein adsorption to the membrane, affects their assembly and dynamics, and ultimately modulates biochemical pathways, as it is described throughout this Review.

Mimetics of macromolecular crowding for *in vitro* studies

Simplified and well-defined model systems allow scrutinizing complex effects of macromolecular crowding. Diverse crowders can be included in biochemical reactions *in vitro* with physiological relevant volume fractions [36]. A good rule of thumb is that the crowder should be smaller than the protein under investigation but much larger than the solvent molecule to obtain the most substantial effects. A common crowder is the synthetic polyethylene glycol (PEG), which is a water-soluble linear polymer available in different sizes. Another common crowder is Ficoll, a chemically cross-linked sucrose-based polymer. Ficoll is well hydrated and usually assumed to be roughly spherical with fewer interactions with biomolecules than PEG. Dextran is a sugar-based polymer with varying degrees of branching, depending on the origin species. Protein-based crowders should be somewhat more relevant to understand *in vivo* crowding as they are able to mimic the surface heterogeneity of biological macromolecules. Inert proteins, like bovine serum albumin (BSA) or lysozyme, can be considered for crowding studies since they are available in the sufficient amounts and can be concentrated to naturally abundant crowding levels [43,49]. However, crowding studies *in vitro* should be interpreted with care. Concentrating crowders may lead to decrease in effective crowder radius [50], or self-association and phase separations [51,52], which are not always easily detectable but can deviate crowding effects. Furthermore, induced effects are often specific for a crowder and may arise from quinary interactions with the molecule under investigation [41], and the complexity in these infarctions as well as the challenges to scrutinize those experimentally have been recently reviewed elsewhere [35,36,53]. Hence, to draw a general conclusion on the effect of crowding, different crowders need to be compared to determine the contributions of the excluded volume and soft interactions.

Synthetic lipid membranes offer a competitive tool to study dynamics of proteins and lipids in a well-defined, although their simplified environment lacks the physiological complexity of protein and lipid composition. Synthetic membranes have been extensively employed to study effects of macromolecular crowding in biochemical and biophysical experiments, and several approaches to mimic abundance of macromolecules have been implemented up to date. As described below, a broad range of studies has been focused on effects of crowding at the membrane interfaces, when anchoring solvent-exposed macromolecules to the membrane surface at varying densities. Different soluble proteins could be docked via specific bonds with functional head groups of synthetic lipids, for example streptavidin:biotin or polyhistidine:Ni^{2+}-NTA interactions [54,55]. Alternatively, commercially available conjugates of PEGs with lipid molecules are reconstituted into lipid bilayers at defined ratios to mimic crowding at the interface [56], while considering that loosely coiled PEG molecules may block protein:

lipid interactions [57] or build up interactions with hydrophobic and nonpolar side chains of solvated proteins [38]. Aiming to study crowding effects within the lipid membrane core, purified integral membrane proteins or detergent-stabilized extracts from cellular membranes are reconstituted into synthetic lipid bilayers at varying densities [58–60], though careful controlling for potential protein aggregation is required. On the other hand, native biological membranes, such as giant plasma membrane vesicles (GPMVs), or isolated organelle membranes can be used to monitor the dynamics of proteins and lipids down to single-molecule level, for example by means of fluorescent microscopy [46,61], but also intact cells with overexpressed membrane proteins have been successfully employed to probe the physiological effects of crowding [62].

In this review, we summarize findings from biochemical, biophysical and computational studies, which show the multifaceted effects of macromolecular crowding on membrane-associated processes. We describe the translational mobility of proteins and lipids within crowded membranes and sum up observations on how the crowding modulates the oligomeric state and clustering of integral membrane proteins. Further, we focus on dynamics of membrane-associated proteins under crowded conditions and specifically address the effects of crowding on membrane transport processes. We also present the most recent findings on the role of crowding-induced entropic forces in shaping the lipid membrane. Finally, we discuss the design and development of fluorescence-based sensors for macromolecular crowding and the perspectives to use those in application to cellular membranes.

Diffusion in crowded membranes and at the interfaces

Two-dimensional diffusion in lipid membranes

Translational mobility of macromolecules determines the kinetics and equilibria of larger complex assembly and interactions of proteins with substrates. The translational mobility of lipids and proteins within the cellular membrane is limited to two-dimensional diffusion, with an exception for relatively rare events of topology inversion. Upon Brownian motion of molecules, their mean square displacement $< r^2 >$ is proportional to time t and the diffusion coefficient D (Fig. 2A). According to Saffman–Delbrück model [47], D of a particle, protein or lipid, within the idealized fluid membrane is largely determined by the viscosity of the membrane ($\mu_m \sim 0.05$–0.1 Pa*s, [63,64]) and weakly influenced by the low viscosity of the surrounding medium. D shows a linear dependence on the depth of embedding into the membrane (h) and a logarithmic dependence on the particle radius (R) (Fig. 2A). The particle radius for the transmembrane protein is determined not only by its own structure, but also by the tightly associated annular lipid shell [65,66]. Validity of Saffman–Delbrück model was experimentally confirmed, for example, by measuring diffusion coefficients of membrane proteins of different sizes of diffusion in homogeneous lipid bilayers at low protein:lipid ratios [58,64].

However, Saffman–Delbrück model does not account for the heterogeneous composition of native cellular membranes and specific protein:lipid contacts, which may occur even in model membranes. For instance, individual membrane proteins change their mobility when forming clusters together with the proximal solvating lipids [66,67]. Changes in the membrane thickness and the associated hydrophobic mismatch between lipids and incorporated proteins can modulate the diffusion behaviour in a complicated manner, up to the transition from a weak dependence $D \sim \ln(1/R)$ to the more pronounced size-dependent Stokes-like diffusion, where $D \sim 1/R$ [45,67–69]. Interactions of the membrane-embedded proteins with the cytoskeleton and confinement induced by protein crowding in cellular membranes further lead to subdiffusion (Fig. 2B). To characterize those deviations from the Brownian diffusion, an anomalous diffusion parameter α is introduced when analysing the molecule displacement (Fig. 2B). For the Brownian diffusion, α equals 1, but it is lower for the confined motion, which is a common case in cellular, but also model membranes. As elaborate descriptions and analyses of diffusion processes in the membrane have been broadly reviewed [45,70–72], we will briefly outline here how macromolecular crowding modulates translational dynamics within the membrane plane.

Macromolecular crowding hinders the lateral mobility in membranes

The effect of a densely packed environment on protein mobility was illustrated by an early study of bacteriorhodopsin in reconstituted liposomes via fluorescence microphotolysis [73]. The diffusion coefficient of the protein was reduced by 20-fold upon increasing the protein:lipid ratio from 1 : 210 up to 1 : 30. The effect could not be assigned solely to changes in the membrane viscosity but implied steric hindrance within the crowded membrane. The conclusion was corroborated by studies *in vivo*. As one example, diffusion of transmembrane and peripherally bound proteins was

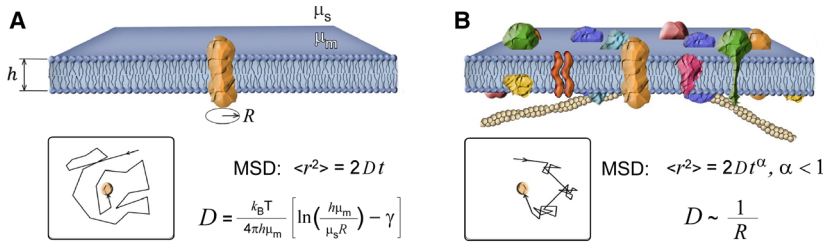

Fig. 2. Non-Brownian diffusion in crowded membranes. (A) A particle (brown) demonstrates Brownian diffusion within an idealized homogeneous membrane, as illustrated by its trajectory (below). The mean square displacement (MSD) of the particle linearly depends on the diffusion coefficient D and time t. Diffusion coefficient D is approximated by the Saffman-Derbruck model and shows a weak logarithmic dependence of the particle size R, but also depends on the viscosity of the membrane (μ_m) and solvent (μ_s) and the depth of the membrane anchoring h. γ is Euler constant. (B) Within the nonhomogeneous and/or crowded membrane, a particle may experience transient confinement events and deviate from Brownian diffusion, so the anomalous diffusion parameter α is below 1. The diffusion coefficient D in the crowded membrane may strongly depend on the particle size.

strongly affected upon changing the membrane protein density in COS-7 cells [74]. More recently, high-sensitivity approaches have made it possible to characterize diffusion in more detail. In particular, diffusion of proteins and lipids in membranes of giant unilamellar vesicles (GUVs) was systematically analysed by fluorescence correlation spectroscopy (FCS) upon varying the protein:lipid ratio [58]. The experiment showed a linear decrease in the diffusion coefficients of several α-helical membrane proteins, but also lipids, upon increasing the protein content. The study suggested a modest contribution of the anomalous diffusion ($\alpha \sim 0.9$) for the highest protein density examined (molar protein:lipid ratio of 1 : 1500) but anticipated further reduction in the mobility upon increasing the protein content towards the naturally occurring levels. GPMVs detached from the cell surface upon a chemical treatment offer a competitive, physiologically relevant mimetic of a cellular membrane [75]. GPMVs are characterized by a high protein content, but lack the membrane-associated cytoskeleton. Diffusion of proteins and lipids within the GPMV membrane is reduced 3- to 5-fold in comparison with GUVs, likely due to the higher protein density [76,77]. However, limited protein:protein and protein:lipid cross-linking upon the GPMV formation may also have an influence on the dynamics and mobility within the membrane [75].

Origins of anomalous diffusion in crowded membranes

Single-molecule imaging techniques, in particular, single-particle tracking (SPT) and high-speed AFM [78–80], reveal further details of lipid and protein diffusion in native and model membranes. Surprisingly, even simple systems, such as a homogeneous lipid membrane, may manifest a substantial dynamic heterogeneity at the single-molecule level: individual lipid molecules were observed in two mobility modes with characteristic diffusion coefficients of 0.07 and 4.4 $\mu m^2/s$, suggesting a nonuniform structure of the membrane, where local 'corrals' areas with a diameter of 100–200 nm exist [78]. Cellular membranes provide a more complex matrix for protein diffusion, where the heterogeneity of the protein and lipid content is accompanied by interactions with the tethered actin cytoskeleton, forming a so-called picket fence structure [17,81,82], and the actin:membrane tether points are commonly associated with densely packed raft nanodomains [83,84]. Protein diffusion in the cellular plasma membrane occurs at lower rates than in corresponding GPMVs, which lack the cytoskeleton [77], and the effect of minimal actin cortex on the lateral diffusion and lipid organization can be reconstituted *in vitro* [85,86]. SPT in native plasma membranes revealed a 'hop diffusion' for proteins trapped within 200–500 nm-sized membrane areas defined by the actin mesh. Proteins were able to cross, or 'hop over' the actin barrier and get into a neighbouring 'cage', and their diffusion was sensitive to the dynamic actin remodelling [81,87,88]. Complementary to fluorescence-based detection, high-speed AFM visualizes single proteins in the native environment down to subnanometer resolution based on variations in their height in time frames below 100 ms [80]. High-speed AFM was employed to characterize lateral movements of label-free outer membrane protein (OMP) OmpF reconstituted in model membranes at a high density, where the proteins occupied ~ 50% of the membrane surface [89]. Distinct diffusion modes were observed for OmpF trimers: a substantial fraction of protein

was found to be nearly immobile and preferentially assembled into large clusters. At the same time, individual porins showed increased displacement velocity up to 15 nm·s^{-1} and could switch between a freely diffusing state and being associated with OmpF clusters. Collisional interactions of individual porins with clusters led to rearrangements within the membrane, and the dynamic heterogeneity in diffusion of single molecules determined a static heterogeneity at the mesoscopic level. Later studies performed with lysenin, a pore-forming protein, revealed up to four distinct diffusion regimes within the densely packed protein arrays at the membrane interface [60]. Lysenins captured by their neighbouring molecules formed a solid and sliding glass-like phase, where proteins can be trapped over several minutes, while the average residence time in the nonhampered state was shorter than 10 s.

Multiple simulation studies on the atomic and coarse-grained levels corroborate the drastic decrease in the lipid and protein mobility upon increasing the protein concentration [90–93]. These studies predict anomalous diffusion and pronounced deviations from Saffman–Delbrück model towards Stokes-like dependence of the diffusion coefficient on the molecular size. Large protein:lipid clusters observed in simulations substantially affect the diffusion: when individual molecules transiently interact with clusters, their mobility is temporarily hindered. The resulting dynamic heterogeneity determines the pronounced Stokes-like diffusion of proteins at the native-like protein:lipid ratios from 1 : 300 and higher [93]. Thus, the mobility of membrane-embedded proteins has a stronger size dependence at the physiological levels of crowding: proteins with smaller radii can neglect the effect of lateral confinement more efficiently in comparison with the larger species, and diffusion of proteins clusters> 10 nm in diameter will be significantly hindered [94]. Reduction in net mobility and an increased contribution of the anomalous diffusion in crowded lipid membranes are also observed for transmembrane β-barrel proteins. Coarse-grained simulations suggested that the diffusion rates of lipids reduced by approximately twofold, from 8 to 4*10^{-7} cm^2·s^{-1}, and the parameter α dropped to 0.8 when the sizable β-barrel OMPs OmpF or FhuA of *E. coli* occupied 40% of the membrane surface area [91]. The lateral mobility of the proteins themselves decreased linearly with the increasing packing density, which could be attributed to transient collisional protein:protein interactions in agreement with experimental observations [89]. Increasing the protein density led to the almost complete immobilization of FhuA because the protein readily formed large clusters, as described in the following chapters.

Formation of densely packed membrane protein clusters raises a challenge for the quality control and repair/degradation of damaged or misfolded proteins, as in the case of the large LHCs in photosynthetic membranes [30,31]. One described recycling mechanism is based on the phosphorylation and disassembly of the damaged complexes within the densely packed regions of grana membranes [95]. Higher mobility of individual subunits allows them to diffuse out of the crowded environment and accumulate at the peripheral grana margins. These highly curved membrane areas are enriched with the quality control components such as Deg and FtsH proteases, which serve for degradation or recycling of the LHC subunits. The nascent LHCs are assembled in the less crowded stroma membrane and localize to the grana upon the lateral diffusion, where they are stably embedded via protein:protein and protein:lipid interactions.

Diffusion of peripheral membrane proteins

Although much less studied, the lateral diffusion of peripheral proteins is also sensitive to the crowding level. According to Saffman–Delbrück model (Fig. 2A), the mobility of peripheral proteins should be higher than for integral membrane proteins, due to limited interactions with the viscous lipid bilayer. Indeed, the diffusion coefficient $D \approx 2$ μm^2/s determined by FCS for the membrane-anchored avidin, a protein of 60 kDa, in a planar lipid bilayer could be compared to that of highly mobile lipid molecules, despite ~ 100-fold difference in their molecular masses [55]. Increasing the avidin density led to anomalous diffusion, once the protein occupied as little as 5% of the membrane surface – a threshold remarkably close to the one observed for integral membrane proteins [58]. The anomalous diffusion parameter approached 0.7 at higher concentrations of avidin, though the enhanced crowding was accompanied with the phase separation at the membrane interface [55]. Diffusion at the crowded membrane interface was further studied by Stachowiak and coworkers [96]. Soluble polyhistidine-tagged proteins of sizes ranging from 5 to 150 kDa were anchored to synthetic Ni^{2+}-NTA chelating lipid groups within the supported lipid bilayer. The protein density could be tuned by changing the abundance of the chelating lipids. Upon switching from the diluted to the densely packed state, an approx. 7-fold decrease in diffusion coefficients was measured by FCS for all

studied proteins. The diffusion coefficients were inversely proportional to the peripheral protein density at the membrane interface rather than the size of the diffusing particle. It must be noted here that increasing the density of macromolecules, such as peripheral proteins or coiled polymers, at one of the membrane leaflets may cause the membrane deformation, either due to changes in the leaflet area upon binding or due to steric repulsion between bulky moieties at the interface. The effects of the peripheral crowding on the membrane morphology *in vitro* and *in vivo* are discussed in details below.

Experimental observations made in diverse model systems confirm that the high density of protein packing within the lipid membrane and at the interface has a prominent effect on the lateral diffusion of proteins, but also lipids. The non-Brownian mobility and decreased diffusion coefficients reflect hindrances for the lateral diffusion due to extensive interactions within the nonhomogeneous crowded membrane or with the proximate cytoskeleton cortex. The membrane complexity causes dynamic heterogeneity of diffusion as individual molecules switch between confined to freely diffusing states. Enhanced transient interactions within the crowded membrane may be important for the assembly of functionally important protein clusters and oligomers, as discussed below.

Quaternary structure of proteins in crowded membranes

The functionality of soluble and membrane proteins often depends on their association into homo- or heterooligomeric complexes. The apparent affinity of the interaction is modulated by naturally occurring crowding via the excluded volume effect and either attractive or repulsive quinary interactions [43]. However, crowding changes the lateral diffusion with an effect on the kinetics of protein complex assembly [97]. The concentration-dependent oligomerization of membrane proteins has been reported in several *in silico* studies for systems composed of lipids and proteins at varying densities, so that the effect of the excluded volume on protein:protein interactions could be examined [91,98,99]. It should be noted though, that similar to 'wet-lab' studies on macromolecular crowding, the developments of computational modelling of those processes are still in their early phase. Thus, suboptimally tuned force fields may result in non-native oligomeric structures and excessive irreversible aggregation of protein in simulated membranes [100,101].

Oligomerization of β-barrel membrane proteins

The simulations of β-barrel proteins from the outer membrane of *E. coli* suggested that their propensity to form clusters within the lipid bilayer varied substantially, being the highest for the iron transporter FhuA [91]. In contrast, the intrinsically trimeric porin OmpF was not able to assemble into higher oligomers in small-scale simulations. However, elongated clusters were reported for the more extensive micrometer-sized membranes [91,102]. The clustering of OMPs was mediated by aromatic and hydrophobic amino acid residues and lacked the specificity in geometry. Therefore, formed oligomers were heterogeneous in protomer orientation, and also clusters of different OMPs could be observed, while transmembrane α-helices (TMHs) were excluded from the interaction [102,103]. Notably, high-resolution imaging of the outer membrane of *E. coli* revealed large proteinaceous 'islands' of 500 nm in diameter. These islands were centred around BAM complexes involved in the insertion of nascent proteins, and they also induced clustering of proteins in the inner membrane *via* proteinaceous bridges [103,104]. The OMP 'islands' diffused passively to the cell poles before the division; hence, these ageing proteins were distributed unequally between daughter cells. Thus, the propensity of OMPs to form large clusters in the crowded membrane could be crucial for the protein turnover in the bacterial outer membranes.

Oligomerization of α-helical membrane proteins

The effects of the crowded environment on protein: protein interactions were experimentally probed for glycophorin A (GpA, single TMH), the abundant membrane protein in RBCs and G protein-coupled receptors (GPCRs, 7 TMHs). GpA oligomerization was studied in RBC-extracted vesicles as a reliable mimic of the cellular membrane [105]. Measuring Förster's resonance energy transfer (FRET) efficiency between fluorescent proteins (FPs) genetically fused to GpA revealed an equilibrium between GpA monomers and dimers. The monomer fraction ranged between 20 and 70%, which depended on GpA expression levels. GpA exists solely as a dimer in detergent micelles and reconstituted proteoliposomes, and hence, the heterologous crowding in cellular membranes reduced the apparent affinity of GpA assembly, and could be a vital factor tuning protein:protein interactions in the lipid environment. This hypothesis was further supported by direct measurements of the GpA dimer stability in membranes [59]. To this end, biotinylated

GpAs were coupled to bulky monovalent streptavidin molecules at the membrane interface, so that only one protomer within a GpA dimer could bind streptavidin. At the same time, the other site on the GpA dimer was not accessible due to the steric overlap. The shielded site occasionally opened by dimer dissociation, so that the dimer kinetic stability determined the efficiency of GpA-biotin:streptavidin assembly. The elegant assay was employed to study whether the GpA dimer was affected by a native-like crowding mimicked by co-reconstituted membrane protein extract from *E. coli*. The experiments revealed a substantial destabilization of GpA dimers by 5 kcal·mol^{-1} when the crowders were present at relatively low protein:lipid mass ratio of 1 : 7. The effect was attributed to competition for the binding surface of GpA with other potential protein partners in the crowded membrane. Those quinary interactions could involve common dimerization motifs, such as GxxxG glycine zippers within TMHs [106]. On the other hand, elevated crowding and large excluded volume within the ER membrane may trigger the oligomerization of Ire1 sensor kinases and promote the unfolded protein response (UPR) [107]. Contacts between the luminal domains of Ire1 protomers mediate the oligomerization of this single-pass membrane protein. Oligomerization is triggered by interactions of Ire1 with unfolded proteins in the ER lumen, but also by the stress within the lipid membrane that attenuates the topology of the amphipathic helix within the kinase [107,108]. A similar effect on the amphipathic helix can be achieved by increasing the apparent protein density in ER, for example, upon the accumulation of saturated lipids and the formation of protein-depleted islands: the islands and the expelled membrane proteins contribute to the excluded volume within the ER membrane and correlate with Ire1 clustering and UPR activation [109].

GPCRs are the most abundant class of eukaryotic membrane receptors with utmost biomedical importance. Their oligomerization has been considered as a general mechanism to tune the signal transduction [110]. In contrast to structural studies, where only monomers of GPCRs have been visualized despite being trapped in different functional states, homo- and heterodimers and higher oligomers have been observed in cellular membranes. GPCRs are often found in segregated clusters within cellular membranes, where their density may influence their quaternary dynamics and function. The abundance levels of GPCRs of different classes may define the balance between homo- and heterooligomers. Coarse-grained simulations of the sphingosine-1-phosphate receptor 1 (S1P1) in a native-like asymmetric lipid membrane revealed rapid dimer formation, which involved approximately 20% of GPCRs [90]. The dimer fraction remained in a dynamic equilibrium with S1P1 monomers along the simulation time, while both symmetric and asymmetric orientation of protomers were observed. FRET-based analysis in simplified liposomal membranes confirmed that formation and dissociation of dimers and higher oligomers is a highly dynamic process, and the association energy is a GPCR-specific parameter that varied between 3.9 kcal·mol^{-1} for β_2-AR adrenergic receptor and −15 kcal·mol^{-1} for cannabinoid receptor type 1 [111]. Importantly, the fraction of homooligomers depended on the density of receptors in the membrane, with an exception for rhodopsin, which could be detected only as a homodimer, which has the lowest association energy. It should be noted that reducing the density of rhodopsin molecules in native rod disk membranes by 50% accelerated the flash response of the receptor by 1.7-fold. Thus, the high-density packing within the specialized membrane suppresses the conformational dynamics, but likely enhances the photon capture efficiency [112].

In brief, the excluded volume generated by transmembrane crowders thus promotes clustering of membrane proteins. Sterically confined proteins may then assemble into functional oligomers of a specific geometry or function within large phase separated clusters [113]. Differently, quinary interactions with crowders are capable to compete with specific protein contacts and greatly reduce their stability. To ensure the efficient protein:protein assembly under natively crowded conditions, specific lipid molecules, such as cardiolipin, cofactors or axillary protein subunits and the cytoskeleton may contribute to the binding interfaces and stabilize functional oligomers in cellular membranes.

Cluster assembly and recognition reactions at the membrane interface

Clustering of dedicated proteins, cadherins and integrins, at focal adhesions within the plasma membrane, is crucial to mediate cell:cell and cell:surface interactions [114]. While the cytoskeleton contributes to the assembly and the stability of these clusters, membrane proteins not involved in the adhesion should be expelled from the contact areas. Similarly, protein segregation takes place within membranes of the immunological synapse. When a contact focus between a T cell and major histocompatibility complexes of an infected cell is built, clustered T-cell receptors cause the local exclusion of other membrane proteins, such as CD45

phosphatase [115,116]. The formed membrane domains enriched with the receptors cannot be categorized as rafts due to the absence of conventional markers, and their assembly principles are not fully understood. A simple mechanism based on crowding and size-dependent protein segregation has been recently derived from a model system, where modular binding and nonbinding proteins were reconstituted into opposing GUVs to study membrane:membrane interactions and protein localization at the interface [117]. The length and the density of reconstituted proteins were altered systematically, and the protein enrichment at the intermembrane contact interface was subsequently quantified. Coupled binding proteins from opposing membranes accumulated at the adhesion interface. Their length, and therefore the intermembrane distance within the adhesion area, set a threshold on the dimensions of nonbinding proteins allowed to partition. Nonbinding proteins, which long extramembrane domains exceeded the intermembrane distance, were largely expelled from the adhesion interface or might be engulfed into the membrane invaginations, once the membrane deformation was possible. This model-based mechanism translates to cellular systems in the example of clustered T-cell receptors and isoforms of CD45 reconstituted into GUVs [118]. Potential lateral *cis*-interactions between the enriched binding proteins [119] and recruitment of specific accessory proteins to the adhesion interfaces further contribute to the excluded volume effect and reduce the accessible area within the adhesion. Therefore, nonbinding proteins are preferentially distributed over the free-standing membrane in a size-dependent manner.

Receptor clustering is mediated by crowding in solution

The postsynaptic density (PSD) within a synapse is another example of a crowded membrane interface, where the ubiquitous receptors of neurotransmitters, such as glutamate, NMDA and AMPA, ensure the transduction of the signal across the membrane to initiate the response cascade (Fig. 3) [120]. Early electron microscopy images visualized PSD as a layer of ~ 25 nm at the cytoplasmic side of the membrane. This layer shows a remarkable contrast due to an anomalously high density of soluble scaffold proteins, such as PSD-95 that interacts with the membrane-embedded receptors. Astonishingly, the density of AMPA receptors within the PSD, which is ~ 1000 molecules·μm^{-2}, exceeds its density in the extrasynaptic membrane by 100-fold [121]. While the receptors demonstrate normal diffusion in the extrasynaptic membrane, their lateral diffusion within the PSD is anomalous, and a significant fraction of receptors are nearly immobile. Potential involvement of macromolecular crowding in retaining the receptors within the functional spot was probed in Monte Carlo simulations [122]. These simulations suggested that increasing the density of unspecific crowders within the PSD leads to the accumulation of AMPA receptors, and their residence time within the PSD may go beyond several hours. Surprisingly, super-resolution fluorescence revealed that, under highly crowded conditions within PSD, scaffold proteins PSD-95 undergo phase separation and form clusters near the synaptic membrane surface [123]. These clusters are ~ 80 nm in diameter and colocalize with membrane domains enriched with AMPA receptors, so PSD-95 may contribute to either the assembly of the membrane domains or their retention within the PSD [124]. Such stabilization of membrane clusters by their soluble counterparts was recently also implied for phase-separated proteasomes at the surface of the ER [125]. In this case, the proteasomes clustered in the ribosome-rich environment and engaged in the processing of membrane-bound substrates. In this manner, the requirements for Cdc48/p97 ATPase were bypassed, but it also suggests that components of ER-associated degradation machinery are colocalized and clustered within the membrane [126]. It also seems plausible that the ubiquitous intrinsically disordered regions (IDRs) within membrane proteins, such as NMDA receptors and various kinases, have a particular contribution to protein oligomerization and clustering under crowded conditions [127,128]. These largely unstructured polypeptides regulate recognition events, receptor-mediated signalling and protein oligomerization. The conformational dynamics of IDRs in a crowded environment have been recently evaluated [36,129]. The conformational flexibility of loosely packed IDRs can be affected by the crowded environment, and their compacted states commonly associated with protein:protein binding may be favoured. However, more complex scenarios cannot be ruled out, as certain intrinsic disordered proteins (IDPs) are insensible to the elevated crowding or may even undergo further crowding-induced destabilization/unfolding [129]. Preservation of their disordered state in crowded environment may be one of the key features for the appropriate functionality maintenance.

Lipid droplet proteome is sensitive to the surface crowding

Binding of peripheral proteins to the membrane is facilitated by weak interactions and may be particularly sensitive to the steric exclusion at the interface

[19]. The case was recently illustrated by studying the proteome dynamics of lipid droplets (LDs). LDs are micrometer-sized intracellular organelles which store neutral lipids, and their solid core is enveloped by a lipid monolayer [130]. The lipid monolayer does not allow the integration of transmembrane proteins but forms an interface for peripheral binding of proteins containing amphipathic helices or apolar anchors. These proteins are often involved in fatty acid and lipid metabolism and mediate LD transformations according to the cellular needs. Among those, CTP-phosphocholine cytidylyltransferase (CCT) mediates PC synthesis during the growth phase of LD. CCT is anchored to the lipid monolayer with an unusually long amphipathic helix (54 amino acid). This contact is lost upon the lipid starvation and LD shrinking, so CCT is released into the cytoplasm and nucleus when its activity is not required. Cellular and reconstituted systems were used to demonstrate that the association of CCT with the LD interface strongly depends on the crowding level at the surface [131]. Shrinking of the available surface area led to higher collision rates with tightly bound proteins, such as lipases and acyltransferases, but also a synthetic mimetic (PEG), resulting in a loss of CCT:monolayer contacts. The crowding at the LD surface could be also tuned by overexpressing enzymes, allowing determination of the competitive protein interactions with the lipid monolayer. The analysis of known structures of LD-associated proteins revealed that hydrophobic helical hairpins ensure tight binding of competing enzymes. At the same time, the affinity of CCT could be enhanced by increasing the length of its amphipathic helix. Therefore, the propensity to anchor at the crowded interfaces may be a LD-specific targeting factor [132].

Hence, steric exclusion and protein clustering at the membrane interface provide simple but efficient tools to orchestrate cellular pathways, from adhesion to signal transduction and metabolism. These physical interactions contribute to the mosaic organization of the biological membranes, together with specific protein:protein and protein:lipid contacts. The described interplay between the membrane organization and the crowding within the proximate aqueous phase also indicates that membrane-associated processes are sensitive to the cellular homeostasis and crowding levels in the cytoplasm, as reviewed in the following sections.

Crowding in solution modulates membrane:protein interactions

Exclusion of molecules from the solvent and their accumulation at the membrane interface may play a key role in their activity and interactions with lipids and membrane-anchored receptors. Several studies demonstrated that localization and condensation of soluble proteins at the lipid membrane interface is sensitive to the macromolecular crowding and, occasionally, phase separation in solution. In a simplified interpretation, the excluded volume in the aqueous phase favours the accumulation of membrane-binding proteins at the membrane interface [133,134]. Their enhanced local concentration promotes protein:lipid and protein:protein interactions, oligomerization and/

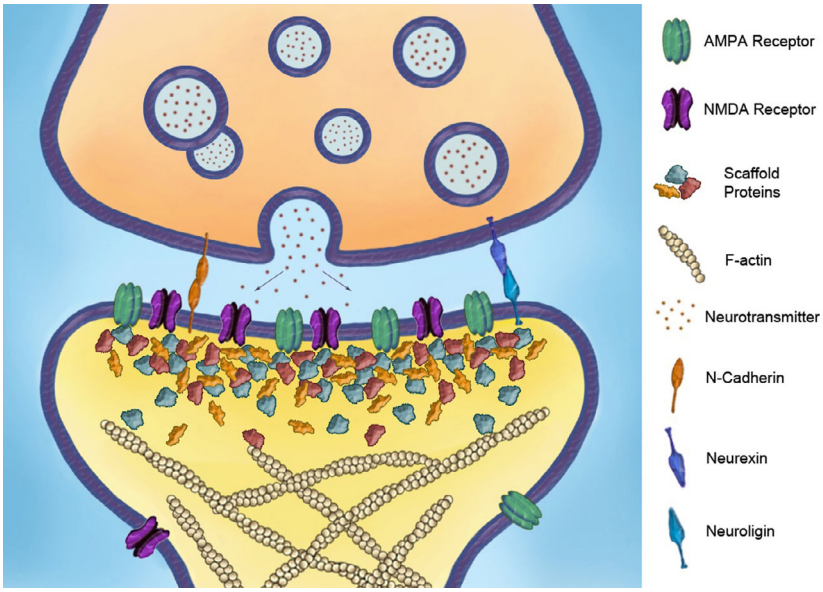

Fig. 3. Crowded environment of the postsynaptic density (PSD). PSD is a dynamic assembly of receptors, scaffold proteins and actin cortex within and proximate to the neuronal postsynaptic membrane. The high density of neurotransmitter (AMPA, NMDA) receptors is a prerequisite for the efficient signal transduction. The receptor density within the PSD is 1000-fold higher that within the plasma membrane. The enrichment and low mobility of receptors within the synaptic membrane is maintained via their interactions with abundant scaffold proteins, such as PSD-95 in the cytoplasm. Thus, macromolecular crowding at the membrane interface induces restructuring within the lipid bilayer.

or aggregation, while soluble proteins and crowders that do not associate with the membrane are largely excluded from the interface [135]. Thus, a twofold higher affinity to lipid vesicles was reported for the phospholipase A1, when as little as 2 % (w/v) of the inert polysaccharide Ficoll 400 was added to the solution [136]. A comparable crowding level imposed by Ficoll PM70 strongly enhanced the virus:receptor recognition on the surface of living cells. In this case, sterically excluded large viral particles accumulated in the proximity to the membrane, while small inhibitor peptides remained distributed in the aqueous phase [137]. Notably, the excluded volume effect recently allowed optimization of the production of universal donor RBCs via enzymatic cleavage of antigen oligosaccharides [138]. The biotechnological process commonly requires substantial amounts of RBC-modifying enzymes, which raises the cost significantly. To increase the concentration of enzymes proximate to the membrane, inert soluble crowders such as Ficoll PM70, dextran and hyperbranched polyglycerol were introduced. Fluorescence imaging confirmed the crowder-dependent accumulation of enzymes on the cell surface, in agreement with the excluded volume effect. As a result, the efficiency of the RBC-modifying enzymes could be increased up to 440-fold [138].

Crowding-dependent assembly of cell division proteins

Protein:lipid interactions and associated membrane remodelling form a basis of cell division. The process has been extensively studied in bacterial systems and shows a remarkable sensitivity to the macromolecular crowding. Bacterial protein FtsZ, a homolog of tubulin essential for the cell division, forms ribbon-like filaments in the presence of polysaccharide crowders, such as dextran and Ficoll. These filaments undergo further phase separation in PEG:dextran and PEG:DNA mixtures [139,140]. A cofactor, DNA-binding protein SlmA mediates the phase separation of FtsZ. Notably, once encapsulated inside lipid vesicles, FtsZ:SlmA condensation occurs mostly at the membrane surface in a GTP-sensitive manner. This localization may be important for the downstream interactions of FtsZ with membrane-associated proteins FtsA and ZapA, as well as the subsequent formation of an active division site in a living cell. Crowding effects may further facilitate the cell division process, as the accumulation of FtsA, a bacterial homolog of actin, at the lipid membrane interface induces membrane instability of liposomes, that is, tubulation and formation of smaller vesicles, in the presence of ATP [141]. Anchoring FtsA to the membrane is mediated by its amphipathic helix, but neither binding alone nor FtsA oligomerization in the absence of ATP causes changes in the lipid membrane morphology. It seems plausible that ATP binding triggers a conformational change within preassembled FtsA clusters, which repositions the amphipathic helices within the scaffolding membrane and provides the deformation force. Whether this membrane remodelling constitutes a natural part of the divisome formation remains to be tested. Complementary insights on membrane-associated crowding have recently been gained by studying oligomerization of another actin homolog, MreB. MreB maintains the elongated shape of bacteria and assembles into aligned filaments in the lumen of liposomes, thus stretching vesicles on the micrometer scale [56]. Similar to FtsA, spontaneous binding of MreB to the lipid leaflet is not sufficient to initiate protein oligomerization. The filament growth is triggered instead by crowding at the membrane interface, as shown by lipid-conjugated PEG polymers as crowders. Oligomerization of membrane-bound MreB was dependent on the size of PEG, ranging between 350 Da and 5 kDa, as well as the density of the polymer on the surface. Once PEG covered the entire surface, filament formation was rapidly abolished because the prerequisite membrane partitioning of MreB cannot occur [142]. It was concluded that the reduction in the accessible surface area stimulates the self-association of the membrane-bound MreB protomers, in agreement with the excluded volume effect. However, more complicated scenarios involving phase separation on the surface before the filament formation cannot be ruled out.

Membrane-associated protein aggregation under crowded conditions

Protein folding and aggregation under native-like crowded conditions have been extensively studied in solution. Under the steric pressure, unfolded polypeptide chains tend to interact with cellular chaperones [143,144], but also aggregate and assemble into fibrils due to compaction into non-native states and enhanced protein:protein interactions [145,146]. Fibrillogenesis is associated with several neurodegenerative diseases mediated by IDPs, such as Aβ, synuclein and prion protein [147]. Interactions of IDPs with membranes containing anionic lipids promote the formation of the secondary structure and contribute to aggregation [148,149]. The theoretical considerations predict that a large exclusion volume in the aqueous phase enhances the IDP association with the lipid

surface. The increased surface density of the proteins would trigger the oligomerization and conversion into β-helical fibres. Indeed, aggregation of Aβ on the surface was enhanced when Ficoll PM 70 was present in solution in concentrations of up to 200 g/L [150]. The aggregation was much reduced at 350 g/L of Ficoll, however, where the elevated viscosity hindered Aβ diffusion and thus shielded the excluded volume effect. A more sophisticated system composed of the synuclein, lipid vesicles and the membrane-associated chaperone Hsp27 was studied by fluorescence anisotropy and single-molecule FRET [151]. As Hsp27 sterically blocked the binding sites on the membrane, it nonspecifically reduced the synuclein accumulation and promoted the soluble form of the IDP. The assay led to a discovery of a bimodal binding of the synuclein to the lipid membrane via its N-terminal and central domains. While Hsp27-induced crowding mainly affected the N-terminal binding, the central part of the synuclein molecule could interact with the lipid leaflet even in the presence of the crowder. The resulting partially folded conformation of the synuclein was resistant to aggregation, suggesting that the abundance of membrane-bound proteins in living cells likely affects the conformational equilibrium of IDPs [151]. Somewhat differently to IDPs, folding of a small, 31 amino acid long zinc finger protein covalently anchored to a lipid monolayer at a high density could not be accomplished, likely due to steric repulsion between otherwise structured domains [152]. Under these crowded conditions and reduced degrees of freedom, the protein acquired partial α-helical fold. The remaining polypeptide chain remained unstructured, possibly in an extended, polymer brush-like conformation. The complete folding of the zinc finger could be restored once a 5-fold excess of lipids was supplied to the monolayer, releasing the steric constraints.

In vitro studies on membrane protein folding are commonly conducted under diluted conditions, to reduce unwanted protein:protein interactions and off-pathway compact intermediates that result in aggregation of the highly hydrophobic proteins. However, β-barrel membrane proteins are usually less hydrophobic, as their transmembrane domains are composed of alternating polar and apolar residues. Therefore, insertion of two OMPs of *E. coli*, OmpA and OmpT, into liposomes was studied to probe the effect of macromolecular crowding [153]. The highly crowded interior of the periplasm that is built from a layer of peptidoglycan, substrate-binding domains of transporters and secretion factors, was mimicked by Ficoll PM70 [154,155]. The presence of 20% Ficoll had no significant effect on the membrane insertion rate of OmpT but reduced the overall efficiency, likely causing some aggregation of the protein. In contrast, the insertion of OmpA approached 100% both in the absence and presence of the crowder. The higher solubility of OmpA was attributed to the chaperoning function of its sizeable periplasmic domain. Notably, the insertion kinetics of OmpA decreased 8-fold in the presence of Ficoll. This decrease was attributed to the excluded volume effect, albeit that the mechanism deserves further investigation. One possible scenario is that the sterically hindered OmpA adopts a compact or an oligomeric form, which undergoes slow conversion and insertion at the membrane interface. As the BAM and chaperoning machinery for OMP targeting and insertion has been described in great detail, probing its functioning and requirements under crowded conditions would be of major interest [104].

Described examples illustrate how dynamics of peripheral proteins at the membrane interface may be affected by macromolecular crowding. The steric exclusion from the solvent causes protein accumulation at the interface and modulates the avidity for the complex assembly or aggregation/phase separation at the interface. Thus, protein localization to the membrane interface depends not only on the intrinsic protein:lipid affinity, but also on the crowding status in the surrounding solvent and at the available membrane surface.

Crowding-mediated transport through biological membranes

The influence of soluble crowders on membrane-associated processes via the steric exclusion plays a fundamental role in the cellular homeostasis. Swelling and shrinking of cells by differences in the osmotic pressure across the membrane alters the concentration of solutes and macromolecules in the cytoplasm. Dedicated cellular systems sense these changes and activate solute transporters and ion channels in the cytoplasmic membrane to restore the osmotic equilibrium. Early experimental data on the volume recovery of RBCs after osmotic stress showed that the albumin content determined the final RBC volume [156]. This implies that the RBC senses the intracellular protein concentration. These data were explained by the function of an ion transporter that set the osmotic strength accordingly. Minton *et al.* provided a theoretical explanation in which the effect of the cytosolic crowding on kinases and their interactions with the membrane proteins within the two-component system was considered based on scaled particle theory [133]. The developed framework suggests that the

kinase:transporter association and the phosphorylation efficiency depend on the concentration of macromolecules in the cytoplasm and the volume they take up. This earlier work provides a tentative two-component pathway for crowding homeostasis.

Conformational dynamics of transporters and channels is mediated by crowding

Direct modulation of the transport activity by crowding has been lately shown for bacterial transporters and channels. Functioning of ATP-binding cassette (ABC) transporters is determined by conformational changes within their bulky ATPase domains exposed to the cytoplasm, where they may be affected by the crowder molecules. Indeed, *in vitro* analysis of a bacterial ABC transporter that couples betaine uptake to ATP hydrolysis revealed its sensitivity to high molecular weight PEGs [157]. The activation profile of the transporter reconstituted into lipid-based nanodiscs shifted to lower ionic strength, and maximum activity was reached at 75 mM KCl when the reaction was supplemented with 8 % PEG 6000. The activation of the transporter is linked to electrostatic interactions within its ATPase domains, so the crowder-induced excluded volume effect counters the electrostatic repulsion between the two lobes of the domain at low ionic strength. The crowding sensitivity was also reported for the secondary transporter ProP, where the proline uptake was significantly stimulated in the presence of either PEG or BSA [158]. The modulation mechanism has not yet been completely understood, but it may involve long C-terminal domains, which activate or regulate osmotically sensitive transporters [158,159]. The C-terminal domain of ProP either forms a coiled-coil with neighbouring protomers or interacts with the lipid bilayer. Macromolecular crowding near the membrane interface may shift this conformational equilibrium, affecting the protein functional response.

Members of a broad class of mechanosensitive channels found in bacteria and eukaryotes switch between closed and open conformations to allow flux of water and ions in response to changes in the membrane tension. The macromolecular crowding near the membrane interface tunes the activity of MscS channel, as crowders interact with the large extramembrane domain of the channel [160]. Another well-studied example, the mechanosensitive channel of large conductance, MscL of *E. coli*, allows rapid efflux of water and aqueous solutes under hypotonic conditions. The channel lacks extramembrane domains, and its gating is achieved by forces within the lipid bilayer. Increasing turgor pressure and the associated tension within the lipid membrane cause tilting of TMHs within the channel in a diaphragm-like fashion, thus opening a sizeable central pore of ~ 25 Å [161]. A theoretical study by Linden and coworkers suggested that the gating-associated expansion of MscL reduces the membrane area available for other proteins and thus contributes to the excluded volume [162]. The associated entropic cost was estimated to be ~ 2 k_BT, which is a remarkably high value in comparison with the gating energy of MscL, which can be as low as 4 k_BT in the lipid bilayer [161]. Although the experimental validation of the crowding-dependent ion currents has yet to be provided, and the net effects involved may be somewhat lower than predicted, it likely remains a factor in the functioning of mechanosensitive channels, both in prokaryotic and eukaryotic cells.

Polymer translocation under crowded conditions

Translocation of unfolded polypeptide chains through cellular membranes is an essential reaction taking place in the cytoplasmic membrane of bacteria and at the surfaces of eukaryotic organelles [163]. Statistical physics analysis suggests that the macromolecular crowding itself may be a driving force for the translocation because extensive steric pressure and repulsive interactions on the *cis*-side of the membrane will target polymer transport through the membrane-embedded pore [164,165]. Once crowders are present on both sides of the membrane, the substrate will predominantly localize in the compartment with larger crowders, as those result in a lower osmotic pressure [166]. However, specific attractive interactions with crowders may have a dominant effect on the direction of the transport [165]. Most recently, protein transport through a membrane-embedded α-haemolysin nanopore with a crowded solution phase was studied experimentally [167]. Haemolysin, a pore-forming bacterial toxin, has extensive use in nanotechnology applications where its wide transmembrane channel allows translocation of synthetic and biopolymers, such as DNA strands and polypeptide chains [168]. Single-channel conductivity of the membrane-embedded haemolysin pores was recorded in the presence of Syn B2, a 23 amino acid long polypeptide, with PEG crowders at both sides of the membrane. Small PEG molecules of 1000 and 2000 Da could partition into the pore and inhibit the protein translocation. Instead, both PEGs 4000 or 8000 kinetically favoured interactions between the haemolysin and the polypeptide. This effect is likely due to the entropic crowding-out of Syn B2 from the solution phase, resulting in trapping the polypeptide within the pore. Notably, PEG 8000 had a weaker effect on

Syn B2:haemolysin association than PEG 6000, which could not solely be explained by the excluded volume. Instead, the observed size dependence was related to the osmotic pressure arising from the small and large crowders, in agreement with the theoretical predictions [166,167], although also different effects of PEGs on diffusion and compaction state of Syn B2 peptide could play a role.

As illustrated above for membrane transport reactions, individual cellular pathways may be sensitive to different and, potentially, additive factors of macromolecular crowding. Membrane and cytosolic crowding may affect conformational dynamics of the transport machinery, but also its macromolecular substrates. Importantly, crowding may be a triggering factor for cellular pathways, for example via two-component system activation at the lipid membrane interface.

Membrane remodelling and fission

Steric repulsion at the interface induces the membrane deformations

Dynamic morphology of cellular membranes, as well as their ability to undergo fusion and fission, is prerequisites for a variety of cellular processes including motility, cytokinesis, vesicle budding and cell signalling [3,169,170]. Changing the membrane shape involves local distortions of the lipid packing, and the arising lateral tension forces should be attenuated to stabilize the new architecture. Because the lipid bilayer packing is determined by structures of lipid head groups and acyl chains, its mechanical properties depend on the lipid composition [171]. These mechanical properties are highly dynamic, as cells tune their lipid composition in response to a changing environment or upon switching between growth phases. Moreover, biological membranes commonly show an asymmetry in the lipid composition between the leaflets, which is built and maintained by lipoactive enzymes and transmembrane flippase proteins and may contribute to the membrane curvature [170]. However, tuning the membrane shape with a high temporal and spatial precision can barely be achieved via restructuring of the cellular lipidome, but instead relies on several protein-based machineries [170,172]. These dedicated soluble proteins insert into the membrane with their amphipathic domains to increase the leaflet area on one side of the membrane. For example, Epsin and Arf proteins bind to the membrane in a crescent-shaped conformation characteristic for Bin/Amphiphysin/Rvs (BAR)-domain containing proteins, and sufficiently strong electrostatic interactions with lipid head groups serve to remodel the bilayer. Oligomerization of the membrane-associated proteins commonly enhances membrane deformation. It stabilizes the altered structure, which is the case for COPI-, COPII- and clathrin-coated vesicles, or bacterial FtsA/FtsZ proteins, as described above [141]. Membrane remodelling by these mechanisms has been extensively studied and could be reproduced *in vitro*, inspiring the engineering of synthetic membrane scaffolds based on DNA origami of varying structures [173].

Complementary to these specialized systems, accumulated experimental evidence indicates that macromolecular crowding shapes lipid membranes *in vitro* and *in vivo*. The membrane-deforming proteins Epsin, with its N-terminal homology domain (ENTH), and Sar1p, did not require amphipathic helices to induce the membrane tubulation and fission once the proteins were anchored at a sufficiently high density at the GUV surface via polyhistidine tags (Fig. 4A,B) [54,174]. Moreover, even the histidine-tagged green fluorescent protein (GFP) and, to a lower extent, mOrange, but not the maltose-binding protein, could induce the formation of thin membrane tubules with a diameter of approximately 28 nm [175,176]. The tubulation effect was assigned to the entropy-based steric repulsion between proteins bound to the lipid bilayer at high density, though protein oligomerization may be also required, as shown for the matrix protein M1 of the influenza A virus [177]. A surface coverage of 20% could be estimated as a minimal threshold for tubulation if proteins were to be considered as hard spheres bound to the elastic membrane. Increasing the crowder size causes a rapid nonlinear stimulation of the tubule growth [54]. In agreement with this, larger crowders, for example, full-length Epsin, are able to induce membrane curvature at a lower coverage density. Comparing two proteins of similar molecular weights, GFP and the N-BAR domain of endophilin, showed that the BAR-induced tubulation required substantially lower protein density, though enhanced membrane remodelling via GFP has been recently reported [178]. However, the moderate effect of the steric pressure between compactly folded proteins on the membrane morphology may vanish when peripherally bound proteins are present at both sides of the cellular membrane [170,176].

Membrane remodelling by disordered biopolymers

More than 40% of human proteins contain IDRs, which include domains in cytoplasmic loops of integral

membrane proteins or membrane-remodelling proteins [128,179]. Experiments on the crowding-induced tubulation revealed that IDRs within Epsin and the adaptor protein AP180 strongly enhanced the membrane remodelling, as it would be expected from the contribution of IDRs to the steric repulsion [54,174,180]. The role of IDRs in membrane tubulation and fission was further investigated using membrane-remodelling proteins amphiphysin and FCHo1/2, in which BAR domains are extended with disordered regions [181]. BAR domains alone caused extensive growth of stable tubules on the surface of large unilamellar vesicles (LUVs). On the other hand, full-length amphiphysin and FCHo1 disintegrated LUVs into highly curved vesicles of 10-fold smaller diameter (20 vs. 200 nm of the intact vesicle). A similar effect was achieved when isolated IDRs were bound to the vesicle surface. Thus, BAR domains stabilize the curved tubular structure of the membrane, while IDR extensions enhance the steric pressure, therefore allowing membrane fission (Fig. 4C). Similar to IDRs, unfolding of lipid-anchored proteins could induce membrane deformations [182]. Anchoring of the folded human serum albumin to the surface of GUVs or liposomes resulted in minor membrane deformations, but enhanced tubulation was induced when the protein was chemically unfolded. Although the experimental evidence does not entirely explain the physiological role of IDPs/IDRs on membrane tubulation and fission in living organisms, it highlights a potential contribution of protein crowding to these processes.

While proteins are highly abundant at the membrane interfaces, other macromolecules may also contribute to crowding. Most recently, a direct connection between the density of the cell surface glycocalyx and the morphology of the plasma membrane was identified [62]. Glycocalyx is built of extensively glycosylated mucin proteins forming 'bottlebrush' structures of up to 20 MDa at the extracellular side of the plasma membrane. Increasing the expression levels of different types of mucin led to the membrane tubulation and shedding of small vesicles, similar to the effect of IDRs described above [181]. These morphological changes were dependent on the glycosylation status of mucins, as enzymatic 'shaving' of polysaccharides caused smoothening of the cell surface. The elevated surface density of glycosylated mucin molecules was recognized as a primary factor

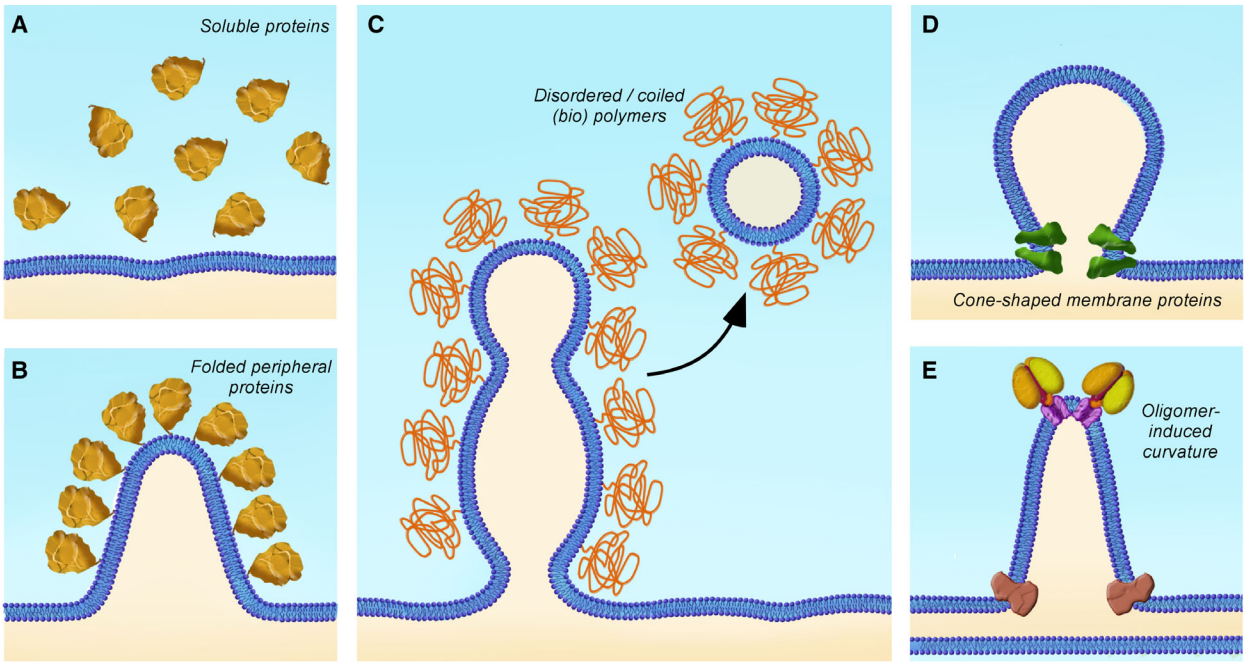

Fig. 4. Membrane remodelling via macromolecular crowding. (A) In the absence of membrane-anchoring domains, soluble proteins are largely excluded from the lipid bilayer interface. (B) Abundant membrane-bound globular proteins cause deformation and tubulation of the lipid bilayer due to entropic forces. (C) Entropy-based tubulation and membrane fission are strongly induced by unstructured synthetic polymers, intrinsically disordered protein domains, and polysaccharides. (D) Cone-shaped membrane proteins cause local membrane deformations and induce vesicle budding. (E) Angular-shaped dimers of the ATP synthase stabilize highly curved structure at the edge of the mitochondrial cristae.

to trigger membrane remodelling, where mucins switched from the 'mushroom' to the 'brush' packing-mode at a concentration 700-1,000 molecules/μm^2. The mucin-covered tubules were stabilized by the actin cytoskeleton, and once the actin was depolymerized, the tubules manifested high elasticity and a propensity to form small vesicles. Because vesicle spreading and extensive tubulations are hallmarks of many cancer cell types, a key role of the enriched glycocalyx and associated membrane morphologies in tumorigenesis was proposed [62].

Densely packed membrane proteins may stabilize membrane curvature

The shape of the membrane is affected by the incorporated proteins [3]. Advances in structural analysis revealed the universe of three-dimensional folds acquired by integral membrane proteins and their complexes, which may strongly deviate from a simplified cylindrical perspective [183]. Because the structure of the proximal lipid bilayer is affected by the protein shape, the intrinsically high and diverse protein content in cellular membranes will considerably contribute to the distribution of the lateral forces [99,184]. Functionally important membrane remodelling has been shown for the matrix protein M2 of influenza A virus [185,186]. The protein is assembled from four individual transmembrane α-helices and is involved in the budding of nascent viral particles without the recruitment of the host ESCRT machinery. Electron paramagnetic resonance-based analysis and simulations suggested that the conical shape of a single M2 protein is sufficient to deform the fluid lipid bilayer locally. The entropy-driven accumulation and clustering of multiple M2 proteins cause mesoscopic membrane deformations towards the scission event (Fig. 4D). Another remarkable example of membrane remodelling by clustered proteins is mitochondrial F_1F_o ATP synthase: its transmembrane domain consists of a highly symmetric ring of F_oc subunits and the F_oa subunit, which forms the passage for protons. This complex can be seen as a cylinder in the membrane [187]. However, within the physiological dimer, ATP synthases are strongly tilted, with an angle ranging between 55 and 90°, thus preventing the steric clash between the sizeable ATPase domains. Notably, the tilt between protomers causes a marked bending of the lipid bilayer, and, once clustered in rows, dimers of the ATP determine the architecture of mitochondrial cristae, stabilizing their sharp edges (Fig. 4E) [188,189].

Steric repulsion at the interface modulates the phase separation within the lipid bilayer

A different feature of crowding-mediated membrane remodelling was reported for phase-separated lipid bilayers [190]. Once peripheral proteins were densely bound within patches of gel-phase lipids in GUVs, they exerted a steric hindrance-induced pressure and caused partial or complete mixing of the initially separated lipid phases. The effect had a clear dependence on the protein size, as transferrin receptors (150 kDa) required 10%, and GFP (26 kDa) 25% of receptor lipids to trigger phase mixing. In contrast, only partial mixing was observed for ubiquitin (5 kDa) even in the presence of 50% receptors. Also, both nanodiscs, which are large discoidal protein:lipid particles, and bulky synthetic polymers bound to phase-separated membranes caused substantial mixing [191,192]. Notably, once the crowders were displaced from the membrane surface by EDTA treatment, the macroscopic phase separation restored within several minutes.

The entropy-driven propensity to remodel the lipid membrane is a unique manifestation of the macromolecular crowding which is only possible within the two-dimensional setting. Bulky and unstructured molecules, either proteins or polysaccharides, accumulated at the lipid bilayer interface cause membrane deformations, such as tubulation and fission. It remains to be shown how the membrane deformation in the presence of crowders correlates with the mechanical properties of the lipid bilayer and also specific crowder:lipid interactions. Nevertheless, results from *in vitro* and *in vivo* studies suggest that the interfacial crowding may sculpture cellular membranes on the macroscopic scale and, together with the cytoskeleton, determine the morphology of living cells.

Quantification of macromolecular crowding

To mimic the physiological macromolecular crowding *in vitro*, quantitative analysis of crowding *in vivo* is required. In principle, cell volume changes [156,193], dry cell mass [33,194], cell buoyant density [195], water content by Raman scattering [196] and other methods provide the solute content of the cytoplasm or the periplasmic space of bacteria. The solute content is less predictive though for the actual magnitude of crowding effects: the cumulative effect depends on the size, shape and surface properties of all molecules involved. Moreover, the magnitude of crowding effects close to the intracellular side of the membrane is mostly unknown, despite its importance for membrane function.

Molecular probes offer complementary insights into the magnitude of macromolecular crowding. For example, diffusion of a fluorescent tracer protein in solution or within the lipid membrane provides information on the macromolecular crowding because the lateral and rotational diffusion decrease upon collisions [197–199]. However, the intrinsic dependence of diffusion on multiple factors, such as confinement or transient interactions with lipids, may hamper the determination of macromolecular crowding. [81,200–202]. Instead, monitoring protein conformation or folding would give insight into the magnitude of the steric exclusion that generally favours polymer compaction, albeit that attractive quinary interactions with the target proteins may diminish the effect of excluded volume [35,41,203–205].

Currently, three probes have been presented that sense the excluded volume from crowding in aqueous solutions. These probes are based on PEG polymers [206], DNA [207] or a disordered polypeptide chain [208]. These are all flexible constructs that compress with increasing macromolecular crowding. The resulting end-to-end distance within the probe is easily measured by FRET, either by conjugation with small-molecule fluorescent dyes or FPs. Thus, the protein probe contains two FPs with a flexible polypeptide linker in between extended with two α-helices (Fig. 5A, B). FPs have little interaction with the cytoplasm, and the α-helices are rigid and well-hydrated to prevent additional interactions. The protein probe has the crucial advantage that it is entirely genetically encoded, allowing expression in many different hosts, genetic fusions with localization tags or other proteins, and manipulation of its structure through genetic engineering. The majority of applications involve this protein-based class of probes, which function in bacteria [208–211], yeast [210,212] and mammalian cell lines [208,213,214], as well as their compartments [210,215]. It allowed crowding determination under stress conditions, such as osmotic stress [211,213] and ageing [212].

What do such probes measure? Various theoretical models and simulations attempt to predict polymer compression induced by macromolecular crowders. No theory captures the experimental observations completely, which is in part a consequence of the conformational complexity of polymers. However, the depletion force is a useful theoretical framework and explains observations at least qualitatively [216–218]. In these terms, the macromolecular crowders do not fit cavities of given protein conformations, leading to spaces depleted of crowder. The difference in osmotic pressure with the crowded medium outside the protein is relieved by compression of the protein, which in turn provides more configurational entropy for the crowders. In another model, scaled particle theory adapted for polymers, the polymer would be placed in a crowded solution, which leads to a decrease in configurational entropy of all the crowders, which also is relieved by polymer compression [219].

Development of the genetically encoded sensors for crowding

To systematically characterize the probe dynamics, a set of nine probes with varied linker composition was recently designed, so the effects of unstructured and α-helical domains were systematically investigated [209]. Inducing crowding with a range of different synthetic polymers and proteins showed that compression of probes is higher with higher crowder concentration and with the size of the crowder until it reaches a plateau at ~ 4 nm radius (the diameters of the probes are in the range of 6–8 nm). Further, the larger the probe, the more it is compressed by crowding. These observations follow partially a scaling law derived from depletion force arguments, where the compression scales with the size of the probe and concentration of the crowders. This theory is not yet complete because the size of the crowder is not yet incorporated correctly. Nonetheless, these probes measure the crowder concentration when the crowders are> 2 nm, freely diffusing, and do not have attractive interactions with the probes.

The expression of the FP-containing probes in cells allows measuring the FRET efficiency and thus the macromolecular crowding *in vivo*. In the absence of an accurate description of the probe conformational dynamics, we content with the comparison of FRET ratios with those obtained in solutions crowded with Ficoll PM70 to indicate the crowding (Fig. 5B,C) [208]. In *E. coli* cells, the cytoplasm crowding is equivalent to ~ 18% w/w Ficoll PM70 and can increase up to 30 % w/w with osmotic upshift of 1 OsM. These values are similar, albeit somewhat lower than biopolymer volume fractions previously determined by cell dry weight. FRET efficiency recorded in HEK293 cells, on the other hand, corresponds to 5 % w/w Ficoll equivalents, so the eukaryotic cytoplasm is less crowded, while a 450 mOsM upshift results in ~ 20 % w/w Ficoll equivalents. Interestingly, the compression of the probes scales with the solute concentration in *E. coli* cells as they do in a crowded buffer, with the caveat that this requires α-helices in the linker of the probes [209]. We hypothesize that the α-helices reduce associative interactions of the linker with the

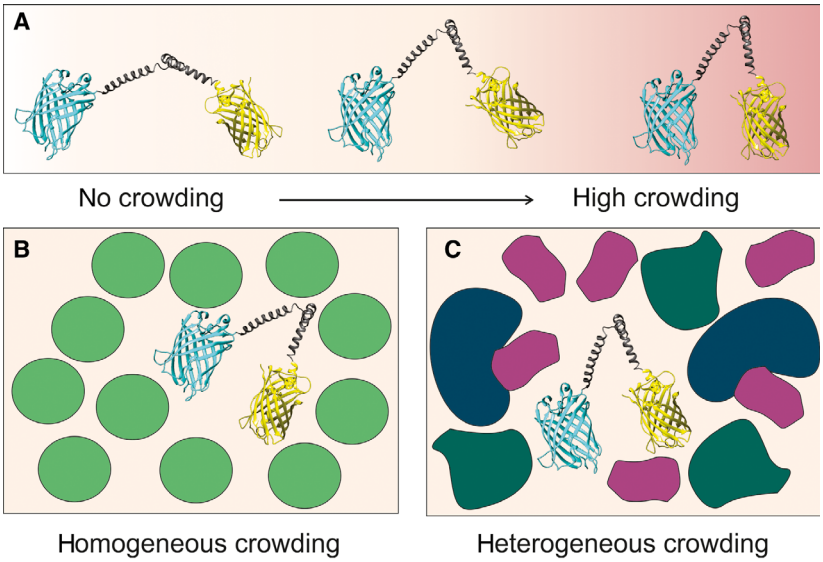

Fig. 5. Compression of a FRET-based macromolecular crowding probe. Genetically encoded probes/sensors of macromolecular crowding rely on measuring Förster's resonance energy transfer between two fluorescent proteins coupled by a semiflexible linker domain. (A) The probe occupies a continuum of conformations that become more condensed on average with increasing macromolecular crowding. Changes in the spatial dimensions and the distance between the fluorescent proteins result in changes in FRET efficiency. Schematic of homogeneously (B) and heterogeneously (C) shaped and sized macromolecular crowders. Both the crowder size and shape affect crowding-sensitive proteins.

proteome. Next to the cytoplasms of the different species, these FP-based probes can be specifically targeted to subcellular compartments, that is, the ER lumen and the nucleus [210,215]. Also, the changes in FRET can be determined by fluorescence lifetime imaging, which provides high resolution and allows untangling putative sensor populations [215,220].

New generations of macromolecular crowding probes with increased robustness allowed better assessment of crowding under challenging conditions, to address questions on how crowding and the biomacromolecular organization changes with environmental stresses, and how the cell responds. To this end, constitutive instead of inducible promoters, as well as faster maturing FPs, overcame artefacts resulting from slow FP maturation [210]. The measurement under these conditions showed that the crowding levels after adaptation of *E. coli* to osmotic stress provided similar, or even slightly lower levels than in unstressed cells [211]. The biopolymer volume fraction was previously determined to be higher in adapted cells, which means that a change in biomacromolecular organization, such as phase separation, must have taken place [221]. A similar conclusion could be drawn by depleting the cells of ATP, suggesting the importance of the organization compared to the total protein content [211].

Substituting the cyan/yellow (mCerulean3 or mTurquoise2/mCitrine or mVenus) FPs for green/red (Clover/Ruby, GFP/mCherry or EGFP/mScarlet-I) provides probes that can be used under less autofluorescence, with less pH sensitivity and allows for more straightforward normalization (N_{FRET}) due to a lower bleed through [212–214]. The probes were applied to study adaptation of mammalian cells to osmotic stress and under the very challenging conditions of yeast replicative ageing [212,213]. The latter experiments tracked the ageing of an individual cell over ~ 2 days, with drifting cell physiology and pH. Here, somewhat surprisingly, the macromolecular crowding is maintained and is even more stable than the difference between individual cells despite an increasing organellar crowding and pH [212]. This observation suggests tight regulation of macromolecular crowding. Altogether, probes for macromolecular crowding under stress conditions strongly suggest that macromolecular crowding is maintained in a window, that is, crowding homeostasis [39].

The advances in the development of the genetically encoded FRET-based probes may be further employed to design probes for measuring crowding at lipid membrane interfaces. Two major challenges here are to target and anchor the probe to the membrane interface in a suitable geometry, and to tune the structure of the probe, so a sufficient sensitivity to the interfacial crowding is achieved. In the simplest scenario, the probe can be docked to NTA-containing liposomes via a polyhistidine tag. However, such design allows only *in vitro* analysis, thus limiting the spectra of applications. One potent strategy would be to express FPs as a fusion with a 'carrier' membrane protein of a known structure, so inter-FP distances can be determined. Here, targeting mechanisms of membrane proteins should be taken into account, as large extramembrane domains within the membrane protein may distort the membrane partitioning and result in aberrant and degradation-prone conformations. Alternatively,

anchoring of the probe can be achieved post-translationally, via moderately hydrophobic domain, such as helical hairpin or Mistic protein [222], fused between FPs. Tuning the composition of the linkers within the probe may minimize their interactions with the lipid head groups. Furthermore, introducing linkers of different lengths may pave the way to measure crowding levels at various distances from the membrane interface deeper in the cytoplasm.

Conclusion and perspectives

Advances in structural and cellular biology witnessed over the last decades have offered insights in molecular mechanisms of membrane proteins and their complexes, but also the overall architecture of cellular membranes [46]. The highly mosaic, asymmetric and heterogeneous compositions of these membranes have indicated that their functionality cannot be described solely by composition deduced from '-omics' approaches, but detailed insights on the spatial and temporal dynamics is essential. Furthermore, the observed high and nonuniform density of proteins within the heterogeneous lipid bilayer and at the interface evidences that macromolecular crowding is an intrinsic feature of the cellular membrane. Two effective mechanisms of crowding are steric exclusion and quinary interactions. The entropy-based steric exclusion favours compaction of individual structures and leads to protein clustering within the lipid bilayer and at the membrane interface. The less predictive quinary interactions can counterbalance these effects. As summarized here, macromolecular crowding affects a broad range of membrane-associated cellular pathways and, next to specific protein:protein and protein:lipid contacts, determines the membrane organization at various scales. Importantly, membrane-associated processes demonstrate a strong dependence on the crowding in the aqueous phase both *in vitro* and in the cytosol of a living cell, as steric exclusion by solute crowders causes protein accumulation at the surface. *Vice versa*, crowding at membrane interface modulates the competitive binding of proteins and may result in protein release back into the aqueous phase. Furthermore, the macroscopic effect of the steric exclusion at the membrane interface is illustrated by extensive membrane remodelling and fission.

Despite the general appreciation of the macromolecular crowding effects, their role in most cellular processes remains to be elucidated. On the one hand, well-characterized cellular pathways should be employed as model systems to evaluate the effects of crowding. One prominent example is the universally conserved Sec pathway for protein translocation and membrane insertion [223]. Here, crowding may affect the initial targeting of polypeptide chains to the membrane by altering their folding state and/or interactions with chaperones, may modulate its interactions with the membrane-embedded protein channel Sec61/SecYEG and may interfere with the assembly of larger complexes between the channel and the accessory chaperones or, occasionally, the degradation machinery. Also interactions of lipoproteins, such as small Ras GTPases, with the membrane may be sensitive to the interfacial crowding [224], and their medically relevant dynamics should be investigated under physiologically relevant conditions. On the other hand, the effects of macromolecular crowding obviously go beyond individual pathways and likely contribute to the global organization of cellular membranes. For instance, formation of phase separated raft nanodomains in the plasma membrane has been largely attributed to protein:lipid interactions, but also the involvement of the actin skeleton has been acknowledged [86,225]. Recent evidences for the effects of interfacial crowding on the lipid phase separation reviewed here point to the potential role of crowding to serve as a regulator for the raft dynamics and their spatial dimensions. Moreover, the crowding effects induced by ubiquitous IDRs within membrane proteins have been barely addressed, although an extensive knowledge on IDR dynamics has been accumulated from studying disordered proteins. The ability of IDPs/IDRs to undergo phase separation in solution further strengthens the potential of membrane crowding to contribute to raft assemblies, although the roles of the steric repulsion and attractive quinary interactions should be examined.

Understanding the dynamics of such multicomponent systems will essentially require a combination of *in vitro*, *in silico* and *in vivo* studies, where different aspects of crowded environment can be assessed in future. Molecular dynamics simulations performed either at the atomic or the coarse-grained level are a powerful tool to study protein interactions, as exemplified by the analysis of densely packed membrane proteins. To get insights on cellular membrane dynamics, dynamics of multiple species of proteins within simulated membranes have to be studied in future, so both steric exclusion and quinary interaction effects are probed. Protein:lipid interactions and the conformational dynamics of proteins at the membrane interface under crowded conditions are among other prominent aims for computational analysis. Real-life experiments need to provide input for *in silico* studies and *vice versa*. Visualization of the native cellular milieu is,

probably, the most direct approach to study the membrane organization. Next to the super-resolution microscopy, cryo-electron tomography (cryo-ET) is rapidly developing into a 'magic bullet' to tackle processes in crowded cellular environments, including those within the cellular membranes [8,226]. With ongoing improvements in its spatial resolution, cryo-ET will help to identify not only the localization and association of macromolecules within a cell, but also their distribution in terms of density and effects of those on the membrane morphology. Quantification of crowding effects, either by diffusion or dedicated sensors, will offer another piece of the puzzle of the crowding effects.

Acknowledgements

We would like to thank Cornelia Monzel, Sander Smits and Stephan Schott for careful reading and commenting on the manuscript. A.K. acknowledges the financial support from the German Research Foundation (Deutsche Forschungsgemeinschaft, DFG) via grants KE1879/3-1 and CRC 1208 'Identity and dynamics of biological membranes' (project number 267205415). A.J.B acknowledges the financial support from The Netherlands Organization for Scientific Research (NWO) VIDI grant 723.015.002.

Conflict of interest

The authors declare no conflict of interest.

Author contribution

All authors contributed to writing and editing the paper.

References

1 Van Meer G, Voelker DR & Feigenson GW (2008) Membrane lipids: Where they are and how they behave. *Nat Rev Mol Cell Biol* **9**, 112–124.
2 Holthuis JCM & Menon AK (2014) Lipid landscapes and pipelines in membrane homeostasis. *Nature* **510**, 48–57.
3 de la Serna JB, Schütz GJ, Eggeling C & Cebecauer M (2016) There is no simple model of the plasma membrane organization. *Front Cell Dev Biol* **4**, 106.
4 Frye LD & Edidin M (1970) The rapid intermixing of cell surface antigens after formation of mouse-human heterokaryons. *J Cell Sci* **7**, 319–335.
5 Singer SJ & Nicolson GL (1972) The fluid mosaic model of the structure of cell membranes. *Science* **175**, 720–731.
6 Harder T, Scheiffele P, Verkade P & Simons K (1998) Lipid domain structure of the plasma membrane revealed by patching of membrane components. *J Cell Biol* **141**, 929–942.
7 Saka SK, Honigmann A, Eggeling C, Hell SW, Lang T & Rizzoli SO (2014) Multi-protein assemblies underlie the mesoscale organization of the plasma membrane. *Nat Commun* **5**, 4509.
8 Beck M & Baumeister W (2016) Cryo-electron tomography: Can it reveal the molecular sociology of cells in atomic detail? *Trends Cell Biol* **26**, 825–837.
9 Fotiadis D (2012) Atomic force microscopy for the study of membrane proteins. *Curr Opin Biotechnol* **23**, 510–515.
10 Engelman DM (2005) Membranes are more mosaic than fluid. *Nature* **438**, 578–580.
11 Laganowsky A, Reading E, Allison TM, Ulmschneider MB, Degiacomi MT, Baldwin AJ & Robinson CV (2014) Membrane proteins bind lipids selectively to modulate their structure and function. *Nature* **510**, 172–175.
12 Shevchenko A & Simons K (2010) Lipidomics: Coming to grips with lipid diversity. *Nat Rev Mol Cell Biol* **11**, 593–598.
13 Goyette J & Gaus K (2017) Mechanisms of protein nanoscale clustering. *Curr Opin Cell Biol* **44**, 86–92.
14 Koler M, Peretz E, Aditya C, Shimizu TS & Vaknin A (2018) Long-term positioning and polar preference of chemoreceptor clusters in *E. coli*. *Nat Commun* **9**, 4444.
15 Sezgin E, Levental I, Mayor S & Eggeling C (2017) The mystery of membrane organization: Composition, regulation and roles of lipid rafts. *Nat Rev Mol Cell Biol* **18**, 361–374.
16 Von Heijne G (2006) Membrane-protein topology. *Nat Rev Mol Cell Biol* **7**, 909–918.
17 Jacobson K, Liu P & Lagerholm BC (2019) The lateral organization and mobility of plasma membrane components. *Cell* **177**, 806–819.
18 Sharpe HJ, Stevens TJ & Munro S (2010) A comprehensive comparison of transmembrane domains reveals organelle-specific properties. *Cell* **142**, 158–169.
19 Johnson JE & Cornell RB (1999) Amphitropic proteins: Regulation by reversible membrane interactions. *Mol Membr Biol* **16**, 217–235.
20 Sahin C, Reid DJ, Marty MT & Landreh M (2020) Scratching the surface: native mass spectrometry of peripheral membrane protein complexes. *Biochem Soc Trans* **48**, 547–558.
21 Itzhak DN, Tyanova S, Cox J & Borner GHH (2016) Global, quantitative and dynamic mapping of protein subcellular localization. *Elife* **5**, e16950.
22 Itzhak DN, Davies C, Tyanova S, Mishra A, Williamson J, Antrobus R, Cox J, Weekes MP & Borner GHH (2017) A mass spectrometry-based

approach for mapping protein subcellular localization reveals the spatial proteome of mouse primary neurons. *Cell Rep* **20**, 2706–2718.
23 Jean Beltran PM, Mathias RA & Cristea IM (2016) A portrait of the human organelle proteome in space and time during cytomegalovirus infection. *Cell Syst* **3**, 361–373.
24 Graham JM (2015) Fractionation of subcellular organelles. *Curr Protoc Cell Biol* **69**, 3.1.1-3.1.22.
25 Dupuy AD & Engelman DM (2008) Protein area occupancy at the center of the red blood cell membrane. *Proc Natl Acad Sci U S A* **105**, 2848–2852.
26 Takamori S, Holt M, Stenius K, Lemke EA, Grønborg M, Riedel D, Urlaub H, Schenck S, Brügger B, Ringler P *et al.* (2006) Molecular anatomy of a trafficking organelle. *Cell* **127**, 831–846.
27 Quinn P, Griffiths G & Warren G (1984) Density of newly synthesized plasma membrane proteins in intracellular membranes II. *Biochemical Studies J Cell Biol* **98**, 2142–2147.
28 Sowers AE & Hackenbrock CR (1981) Rate of lateral diffusion of intramembrane particles: Measurement by electrophoretic displacement and rerandomization. *Proc Natl Acad Sci U S A* **78**, 6246–6250.
29 Fotiadis D, Liang Y, Filipek S, Saperstein DA, Engel A & Palczewski K (2003) Rhodopsin dimers in native disc membranes. *Nature* **421**, 127–128.
30 Kirchhoff H (2008) Molecular crowding and order in photosynthetic membranes. *Trends Plant Sci* **13**, 201–207.
31 Liu LN & Scheuring S (2013) Investigation of photosynthetic membrane structure using atomic force microscopy. *Trends Plant Sci* **18**, 277–286.
32 Fulton AB (1982) How crowded is the cytoplasm? *Cell* **30**, 345–347.
33 Zimmerman SB & Trach SO (1991) Estimation of macromolecule concentrations and excluded volume effects for the cytoplasm of Escherichia coli. *J Mol Biol* **222**, 599–620.
34 Ellis RJ (2001) Macromolecular crowding: Obvious but underappreciated. *Trends Biochem Sci* **26**, 597–604.
35 Sarkar M, Li C & Pielak GJ (2013) Soft interactions and crowding. *Biophys Rev* **5**, 187–194.
36 Kuznetsova IM, Turoverov KK & Uversky VN (2014) What macromolecular crowding can do to a protein. *Int J Mol Sci* **15**, 23090–23140.
37 Wang Y, Li C & Pielak GJ (2010) Effects of proteins on protein diffusion. *J Am Chem Soc* **132**, 9392–9397.
38 Zhou H-X, Rivas G & Minton AP (2008) Macromolecular crowding and confinement: biochemical, biophysical, and potential physiological consequences. *Annu Rev Biophys* **37**, 375–397.
39 Van Den Berg J, Boersma AJ & Poolman B (2017) Microorganisms maintain crowding homeostasis. *Nat Rev Microbiol* **15**, 309–318.
40 Wang Y, Sarkar M, Smith AE, Krois AS & Pielak GJ (2012) Macromolecular crowding and protein stability. *J Am Chem Soc* **134**, 16614–16618.
41 Monteith WB, Cohen RD, Smith AE, Guzman-Cisneros E & Pielak GJ (2015) Quinary structure modulates protein stability in cells. *Proc Natl Acad Sci U S A* **112**, 1739–1742.
42 Sarkar M, Lu J & Pielak GJ (2014) Protein-crowder charge and protein stability. *Biochemistry* **53**, 1601–1606.
43 Guseman AJ, Perez Goncalves GM, Speer SL, Young GB & Pielak GJ (2018) Protein shape modulates crowding effects. *Proc Natl Acad Sci U S A* **115**, 10965–10970.
44 Grasberger B, Minton AP, DeLisi C & Metzger H (1986) Interaction between proteins localized in membranes. *Proc Natl Acad Sci U S A* **83**, 6258–6262.
45 Guigas G & Weiss M (2016) Effects of protein crowding on membrane systems. *Biochim Biophys Acta – Biomembr* **1858**, 2441–2450.
46 Lorent JH, Levental KR, Ganesan L, Rivera-Longsworth G, Sezgin E, Doktorova M, Lyman E, Levental I (2020) Plasma membranes are asymmetric in lipid unsaturation, packing and protein shape. *Nat Chem Biol* **16**, 644–652. http://doi.org/10.1038/s41589-020-0529-6
47 Saffman PG & Delbrück M (1975) Brownian motion in biological membranes. *Proc Natl Acad Sci U S A* **72**, 3111–3113.
48 Surma MA, Klose C & Simons K (2012) Lipid-dependent protein sorting at the trans-Golgi network. *Biochim Biophys Acta – Mol Cell Biol Lipids* **1821**, 1059–1067.
49 Li C, Wang Y & Pielak GJ (2009) Translational and rotational diffusion of a small globular protein under crowded conditions. *J Phys Chem B* **113**, 13390–13392.
50 Wenner JR & Bloomfield VA (1999) Crowding effects on EcoRV kinetics and binding. *Biophys J* **77**, 3234–3241.
51 Levi V & González Flecha FL (2002) Reversible fast-dimerization of bovine serum albumin detected by fluorescence resonance energy transfer. *Biochim Biophys Acta – Proteins Proteomics* **1599**, 141–148.
52 Alberti S, Saha S, Woodruff JB, Franzmann TM, Wang J & Hyman AA (2018) A user's guide for phase separation assays with purified proteins. *J Mol Biol* **430**, 4806–4820.
53 Kuznetsova IM, Zaslavsky BY, Breydo L, Turoverov KK & Uversky VN (2015) Beyond the excluded volume effects: mechanistic complexity of the crowded milieu. *Molecules* **20**, 1377–1409.
54 Stachowiak JC, Schmid EM, Ryan CJ, Ann HS, Sasaki DY, Sherman MB, Geissler PL, Fletcher DA & Hayden CC (2012) Membrane bending by protein-protein crowding. *Nat Cell Biol* **14**, 944–949.

55 Horton MR, Höfling F, Rädler JO & Franosch T (2010) Development of anomalous diffusion among crowding proteins. *Soft Matter* **6**, 2648–2656.
56 Garenne D, Libchaber A & Noireaux V (2020) Membrane molecular crowding enhances MreB polymerization to shape synthetic cells from spheres to rods. *Proc Natl Acad Sci U S A* **117**, 1902–1909.
57 Immordino ML, Dosio F & Cattel L (2006) Stealth liposomes : review of the basic science, rationale, and clinical applications, existing and potential. *Int J Nanomedicine* **1**, 297–315.
58 Ramadurai S, Holt A, Krasnikov V, Van Den Bogaart G, Killian JA & Poolman B (2009) Lateral diffusion of membrane proteins. *J Am Chem Soc* **131**, 12650–12656.
59 Hong H & Bowie JU (2011) Dramatic destabilization of transmembrane helix interactions by features of natural membrane environments. *J Am Chem Soc* **133**, 11389–11398.
60 Munguira I, Casuso I, Takahashi H, Rico F, Miyagi A, Chami M & Scheuring S (2016) Glasslike membrane protein diffusion in a crowded membrane. *ACS Nano* **10**, 2584–2590.
61 Schneider F, Waithe D, Clausen MP, Galiani S, Koller T, Ozhan G, Eggeling C & Sezgin E (2017) Diffusion of lipids and GPI-anchored proteins in actin-free plasma membrane vesicles measured by STED-FCS. *Mol Biol Cell* **28**, 1507–1518.
62 Shurer CR, Kuo JC, Feigenson GW, Reesink HL, Paszek MJ, Gandhi JG & Colville MJ (2019) Physical principles of membrane shape regulation by the glycocalyx. *Cell* **177**, 1757–1770.
63 Vaz WLC, Goodsaid-Zalduondo F & Jacobson K (1984) Lateral diffusion of lipids and proteins in bilayer membranes. *FEBS Lett* **174**, 199–207.
64 Weiß K, Neef A, Van Q, Kramer S, Gregor I & Enderlein J (2013) Quantifying the diffusion of membrane proteins and peptides in black lipid membranes with 2-focus fluorescence correlation spectroscopy. *Biophys J* **105**, 455–462.
65 Lee AG (2004) How lipids affect the activities of integral membrane proteins. *Biochim Biophys Acta – Biomembr* **1666**, 62–87.
66 Niemela PS, Miettinen MS, Monticelli L, Hammaren H, Bjelkmar P, Murtola T, Lindahl E & Vattulainen I (2010) Membrane proteins diffuse as dynamic complexes with lipids. *J Am Chem Soc* **132**, 7574–7575.
67 Camley BA & Brown FLH (2012) Contributions to membrane-embedded-protein diffusion beyond hydrodynamic theories. *Phys Rev E – Stat Nonlinear Soft Matter Phys* **85**, 23–25.
68 Naji A, Levine AJ & Pincus PA (2007) Corrections to the Saffman-Delbrück mobility for membrane bound proteins. *Biophys J* **93**, L49–L51.
69 Gambin Y, Lopez-Esparza R, Reffay M, Sierecki E, Gov NS, Genest M, Hodges RS & Urbach W (2006) Lateral mobility of proteins in liquid membranes revisited. *Proc Natl Acad Sci U S A* **103**, 2098–2102.
70 Chiantia S, Ries J & Schwille P (2009) Fluorescence correlation spectroscopy in membrane structure elucidation. *Biochim Biophys Acta – Biomembr* **1788**, 225–233.
71 Höfling F & Franosch T (2013) Anomalous transport in the crowded world of biological cells. *Reports Prog Phys* **76**, 1–55.
72 Marrink SJ, Corradi V, Souza PCT, Ingólfsson HI, Tieleman DP & Sansom MSP (2019) Computational modeling of realistic cell membranes. *Chem Rev* **119**, 6184–6226.
73 Peters R & Cherry RJ (1982) Lateral and rotational diffusion of bacteriorhodopsin in lipid bilayers: experimental test of the Saffman-Delbruck equations. *Proc Natl Acad Sci U S A* **79**, 4317–4321.
74 Frick M, Schmidt K & Nichols BJ (2007) Modulation of lateral diffusion in the plasma membrane by protein density. *Curr Biol* **17**, 462–467.
75 Levental KR & Levental I (2015) Giant plasma membrane vesicles: models for understanding membrane organization. *Curr Top Membr* **75**, 25–57.
76 Sezgin E, Levental I, Grzybek M, Schwarzmann G, Mueller V, Honigmann A, Belov VN, Eggeling C, Coskun Ü, Simons K *et al.* (2012) Partitioning, diffusion, and ligand binding of raft lipid analogs in model and cellular plasma membranes. *BBA – Biomembr* **1818**, 1777–1784.
77 Worch R, Petrasek Z, Schwille P & Weidemann T (2017) Diffusion of single-pass transmembrane receptors: from the plasma membrane into giant liposomes. *J Membr Biol* **250**, 393–406.
78 Saxton MJ & Jacobson K (1997) Single-particle tracking: applications to membrane dynamics. *Annu Rev Biophys Biomol Struct* **26**, 373–399.
79 Ritchie K, Shan XY, Kondo J, Iwasawa K, Fujiwara T & Kusumi A (2005) Detection of non-Brownian diffusion in the cell membrane in single molecule tracking. *Biophys J* **88**, 2266–2277.
80 Heath GR & Scheuring S (2019) Advances in high-speed atomic force microscopy (HS-AFM) reveal dynamics of transmembrane channels and transporters. *Curr Opin Struct Biol* **57**, 93–102.
81 Ritchie K, Iino R, Fujiwara T, Murase K, Kusumi A, Ritchie K, Iino R, Fujiwara T & Murase K (2003) The fence and picket structure of the plasma membrane of live cells as revealed by single molecule techniques. *Mol Membr Biol* **20**, 13–18.
82 Vogel SK, Greiss F, Khmelinskaia A & Schwille P (2017) Control of lipid domain organization by a biomimetic contractile actomyosin cortex. *Elife* **6**, e24350.

83 Chichili GR & Rodgers W (2009) Cytoskeleton – membrane interactions in membrane raft structure. *Cell Mol Life Sci* **66**, 2319–2328.

84 Lillemeier BF, Pfeiffer JR, Surviladze Z, Wilson BS & Davis MM (2006) Plasma membrane-associated proteins are clustered into islands attached to the cytoskeleton. *Proc Natl Acad Sci U S A* **103**, 18992–18997.

85 Heinemann F, Vogel SK & Schwille P (2013) Lateral membrane diffusion modulated by a minimal actin cortex. *Biophys J* **104**, 1465–1475.

86 Honigmann A, Sadeghi S, Keller J, Hell SW, Eggeling C & Vink R (2014) A lipid bound actin meshwork organizes liquid phase separation in model membranes. *Elife* **2014**, e01671.

87 He W, Song H, Su Y, Geng L, Ackerson BJ, Peng HB & Tong P (2016) Dynamic heterogeneity and non-Gaussian statistics for acetylcholine receptors on live cell membrane. *Nat Commun* **7**, 11701.

88 Andrews NL, Lidke KA, Pfeiffer JR, Burns AR, Wilson BS, Oliver JM & Lidke DS (2008) Actin restricts FceRI diffusion and facilitates antigen-induced receptor immobilization. *Nat Cell Biol* **10**, 955–963.

89 Casuso I, Khao J, Chami M, Paul-Gilloteaux P, Husain M, Duneau JP, Stahlberg H, Sturgis JN & Scheuring S (2012) Characterization of the motion of membrane proteins using high-speed atomic force microscopy. *Nat Nanotechnol* **7**, 525–529.

90 Koldsø H & Sansom MSP (2015) Organization and dynamics of receptor proteins in a plasma membrane. *J Am Chem Soc* **137**, 14694–14704.

91 Goose JE & Sansom MSP (2013) Reduced lateral mobility of lipids and proteins in crowded membranes. *PLoS Comput Biol* **9**, e1003033.

92 Jeon J-H, Javanainen M, Martinez-Seara H, Metzler R & Vattulainen I (2016) Protein crowding in lipid bilayers gives rise to Non-Gaussian anomalous lateral diffusion of phospholipids and proteins. *Phys Rev X* **6**, 021006.

93 Javanainen M, Martinez-Seara H, Metzler R & Vattulainen I (2017) Diffusion of integral membrane proteins in protein-rich membranes. *J. Phys Chem Lett* **8**, 4308–4313.

94 Guigas G & Weiss M (2008) Influence of hydrophobic mismatching on membrane protein diffusion. *Biophys J* **95**, 25–27.

95 Puthiyaveetil S, Tsabari O, Lowry T, Lenhert S, Lewis RR, Reich Z & Kirchhoff H (2014) Compartmentalization of the protein repair machinery in photosynthetic membranes. *Proc Natl Acad Sci U S A* **111**, 15839–15844.

96 Houser JR, Busch DJ, Bell DR, Li B, Ren P & Stachowiak JC (2016) The impact of physiological crowding on the diffusivity of membrane bound proteins. *Soft Matter* **12**, 2127–2134.

97 Zhou H-X (2009) Crowding effects of membrane proteins. *J Phys Chem B* **113**, 7995–8005.

98 Domański J, Marrink SJ & Schäfer LV (2012) Transmembrane helices can induce domain formation in crowded model membranes. *Biochim Biophys Acta – Biomembr* **1818**, 984–994.

99 Duncan AL, Reddy T, Koldsø H, Hélie J, Fowler PW, Chavent M & Sansom MSP (2017) Protein crowding and lipid complexity influence the nanoscale dynamic organization of ion channels in cell membranes. *Sci Rep* **7**, 16647.

100 Javanainen M, Martinez-Seara H & Vattulainen I (2017) Excessive aggregation of membrane proteins in the Martini model. *PLoS One* **12**, e0187936.

101 Alessandri R, Souza PCT, Thallmair S, Melo MN, De Vries AH & Marrink SJ (2019) Pitfalls of the Martini model. *J Chem Theory Comput* **15**, 5448–5460.

102 Chavent M, Duncan AL, Rassam P, Birkholz O, Hélie J, Reddy T, Beliaev D, Hambly B, Piehler J, Kleanthous C *et al.* (2018) How nanoscale protein interactions determine the mesoscale dynamic organisation of bacterial outer membrane proteins. *Nat Commun* **9**, 2846.

103 Rassam P, Copeland NA, Birkholz O, Tóth C, Chavent M, Duncan AL, Cross SJ, Housden NG, Kaminska R, Seger U *et al.* (2015) Supramolecular assemblies underpin turnover of outer membrane proteins in bacteria. *Nature* **523**, 333–336.

104 Rollauer SE, Sooreshjani MA, Noinaj N & Buchanan SK (2015) Outer membrane protein biogenesis in Gram-negative bacteria. *Philos Trans B* **370**, 1–10.

105 Chen L, Novicky L, Merzlyakov M, Hristov T & Hristova K (2010) Measuring the energetics of membrane protein dimerization in mammalian membranes. *J Am Chem Soc* **132**, 3628–3635.

106 Moore DT, Berger BW & DeGrado WF (2008) Protein-protein interactions in the membrane: sequence, structural, and biological motifs. *Structure* **16**, 991–1001.

107 Covino R, Hummer G & Ernst R (2018) Review integrated functions of membrane property sensors and a hidden side of the unfolded protein response. *Mol Cell* **71**, 458–467.

108 Volmer R, Van Der Ploeg K & Ron D (2013) Membrane lipid saturation activates endoplasmic reticulum unfolded protein response transducers through their transmembrane domains. *Proc Natl Acad Sci U S A* **110**, 4628–4633.

109 Shen Y, Zhao Z, Zhang L, Shi L, Shahriar S, Chan RB, DI Paolo G & Min W (2017) Metabolic activity induces membrane phase separation in endoplasmic reticulum. *Proc Natl Acad Sci U S A* **114**, 13394–13399.

110 Milligan G, Ward RJ & Marsango S (2019) GPCR homo-oligomerization. *Curr Opin Cell Biol* **57**, 40–47.

111 Walsh SM, Mathiasen S, Christensen SM, Fay JF, King C, Provasi D, Borrero E, Rasmussen SGF, Fung JJ, Filizola M *et al.* (2018) Single proteoliposome high-content analysis reveals differences in the homo-oligomerization of GPCRs. *Biophys J* **115**, 300–312.
112 Calvert PD, Govardovskii VI, Krasnoperova N & Anderson RE (2001) Membrane protein diffusion sets the speed of rod phototransduction. *Nature* **411**, 90–94.
113 Heinkel F, Abraham L, Ko M, Chao J, Bach H, Hui LT, Li H, Zhu M, Ling YM, Rogalski JC *et al.* (2019) Phase separation and clustering of an ABC transporter in Mycobacterium tuberculosis. *Proc Natl Acad Sci U S A* **116**, 16326–16331.
114 Kechagia JZ, Ivaska J & Roca-Cusachs P (2019) Integrins as biomechanical sensors of the microenvironment. *Nat Rev Mol Cell Biol* **20**, 457–473.
115 Douglass AD & Vale RD (2005) Single-molecule microscopy reveals plasma membrane microdomains created by protein-protein networks that exclude or trap signaling molecules in T cells. *Cell* **121**, 937–950.
116 James JR & Vale RD (2012) Biophysical mechanism of T-cell receptor triggering in a reconstituted system. *Nature* **487**, 64–69.
117 Schmid EM, Bakalar MH, Choudhuri K, Weichsel J, Ann HS, Geissler PL, Dustin ML & Fletcher DA (2016) Size-dependent protein segregation at membrane interfaces. *Nat Phys* **12**, 704–711.
118 Carbone CB, Kern N, Fernandes RA, Hui E & Su X (2017) In vitro reconstitution of T cell receptor-mediated segregation of the CD45 phosphatase. *Proc Natl Acad Sci U S A* E9338–E9345.
119 Fenz SF, Bihr T, Schmidt D, Merkel R, Seifert U, Sengupta K & Smith AS (2017) Membrane fluctuations mediate lateral interaction between cadherin bonds. *Nat Phys* **13**, 906–913.
120 Chen X, Winters C, Azzam R, Li X, Galbraith JA, Leapman RD & Reese TS (2008) Organization of the core structure of the postsynaptic density. *Proc Natl Acad Sci U S A* **105**, 4453–4458.
121 Tanaka JI, Matsuzaki M, Tarusawa E, Momiyama A, Molnar E, Kasai H & Shigemoto R (2005) Number and density of AMPA receptors in single synapses in immature cerebellum. *J Neurosci* **25**, 799–807.
122 Santamaria F, Gonzalez J, Augustine GJ & Raghavachari S (2010) Quantifying the effects of elastic collisions and non- covalent binding on glutamate receptor trafficking in the post-synaptic density. *PLoS Comput Biol* **6**, e1000780.
123 MacGillavry HD, Song Y, Raghavachari S & Blanpied TA (2013) Nanoscale scaffolding domains within the postsynaptic density concentrate synaptic ampa receptors. *Neuron* **78**, 615–622.
124 Li TP, Song Y, Macgillavry HD, Blanpied TA & Raghavachari S (2016) Protein crowding within the postsynaptic density can impede the escape of membrane proteins. *Journal Neurosci* **36**, 4276–4295.
125 Albert S, Wietrzynski W, Lee C, Schaffer M, Beck F, Schuller JM, Salome PA, Plitzko JM, Baumeister W & Engel BD (2020) Direct visualization of degradation microcompartments at the ER membrane. *Proc Natl Acad Sci U S A* **117**, 1069–1080.
126 Ruggiano A, Foresti O & Carvalho P (2014) ER-associated degradation: protein quality control and beyond. *J Cell Biol* **204**, 869–879.
127 Uversky VN (2011) Multitude of binding modes attainable by intrinsically disordered proteins : a portrait gallery of disorder-based complexes. *Chem Soc Rev* **40**, 1623–1634.
128 Kjaergaard M & Kragelund BB (2017) Functions of intrinsic disorder in transmembrane proteins. *Cell Mol Life Sci* **74**, 3205–3224.
129 Fonin AV, Darling AL, Kuznetsova IM, Turoverov KK & Uversky VN (2018) Intrinsically disordered proteins in crowded milieu : when chaos prevails within the cellular gumbo. *Cell Mol Life Sci* **75**, 3907–3929.
130 Olzmann JA & Carvalho P (2019) Dynamics and functions of lipid droplets. *Nat Rev Mol Cell Biol* **20**, 137–155.
131 Kory N, Thiam A, Farese RV & Walther TC (2015) Protein crowding is a determinant of lipid droplet protein composition. *Dev Cell* **34**, 351–363.
132 Prévost C, Sharp ME, Kory N, Lin Q, Voth GA, Farese RVJ & Walther TC (2018) Mechanism and determinants of amphipathic helix-containing protein targeting to lipid droplets. *Dev Cell* **44**, 73–86.
133 Minton AP, Colclasuret GC & Parkert JC (1992) Model for the role of macromolecular crowding in regulation of cellular volume. *Proc Natl Acad Sci U S A* **89**, 10504–10506.
134 Kim JS & Yethiraj A (2010) Crowding effects on association reactions at membranes. *Biophys J* **98**, 951–958.
135 Nawrocki G, Im W, Sugita Y & Feig M (2019) Clustering and dynamics of crowded proteins near membranes and their influence on membrane bending. *Proc Natl Acad Sci U S A* **116**, 24562–24567.
136 Wei Y, Mayoral-Delgado I, Stewart NA & Dymond MK (2019) Macromolecular crowding and membrane binding proteins: the case of phospholipase A1. *Chem Phys Lipids* **218**, 91–102.
137 Rincon V, Bocanegra R, Rodriguez-Huete A, Rivas G & Mateu MG (2011) Effects of macromolecular crowding on the inhibition of virus assembly and virus-cell receptor recognition. *Biophys J* **100**, 738–746.
138 Chapanian R, Kwan DH, Constantinescu I, Shaikh FA, Rossi NAA, Withers SG & Kizhakkedathu JN (2014) Enhancement of biological reactions on cell

surfaces via macromolecular crowding. *Nat Commun* **5**, 4683.
139 González JM, Jiménez M, Vélez M, Mingorance J, Andreu JM, Vicente M & Rivas G (2003) Essential cell division protein FtsZ assembles into one monomer-thick ribbons under conditions resembling the crowded intracellular environment. *J Biol Chem* **278**, 37664–37671.
140 Monterroso B, Zorrilla S, Sobrinos-Sanguino M, Robles-Ramos MA, López-Álvarez M, Margolin W, Keating CD & Rivas G (2019) Bacterial FtsZ protein forms phase-separated condensates with its nucleoid-associated inhibitor SlmA. *EMBO Rep* **20**, e45946.
141 Conti J, Viola MG & Camberg JL (2018) FtsA reshapes membrane architecture and remodels the Z-ring in *Escherichia coli*. *Mol Microbiol* **107**, 558–576.
142 Pozzi D, Colapicchioni V, Caracciolo G, Piovesana S, Capriotti AL, Palchetti S, De Grossi S, Riccioli A, Amenitsch H & Laganà A (2014) Effect of polyethyleneglycol (PEG) chain length on the bio-nano- interactions between PEGylated lipid nanoparticles and biological fluids: From nanostructure to uptake in cancer cells. *Nanoscale* **6**, 2782–2792.
143 Martin J & Hartl FU (1997) The effect of macromolecular crowding on chaperonin-mediated protein folding. *Proc Natl Acad Sci U S A* **94**, 1107–1112.
144 Kulothungan SR, Das M, Johnson M, Ganesh C & Varadarajan R (2009) Effect of crowding agents, signal peptide, and chaperone secb on the folding and aggregation of e. coli maltose binding protein. *Langmuir* **25**, 6637–6648.
145 Munishkina LA, Ahmad A, Fink AL & Uversky VN (2008) Guiding protein aggregation with macromolecular crowding. *Biochemistry* **47**, 8993–9006.
146 White DA, Buell AK, Knowles TPJ, Welland ME & Dobson CM (2010) Protein aggregation in crowded environments. *J Am Chem Soc* **132**, 5170–5175.
147 Uversky VN, Oldfield CJ & Dunker AK (2008) Intrinsically disordered proteins in human diseases: introducing the D 2 concept. *Annu Rev Biophys* **37**, 215–246.
148 Bokvist M, Lindström F, Watts A & Gröbner G (2004) Two types of Alzheimer's β-Amyloid (1–40) peptide membrane interactions: aggregation preventing transmembrane anchoring versus accelerated surface fibril formation. *J Mol Biol* **335**, 1039–1049.
149 Dikiy I & Eliezer D (2012) Folding and misfolding of alpha-synuclein on membranes. *Biochim Biophys Acta – Biomembr* **1818**, 1013–1018.
150 Bokvist M & Grobner G (2007) Misfolding of amyloidogenic protein at membrane surfaces: impact of macromolecular crowding. *J Am Chem. Soc* **129**, 14848–14849.
151 Banerjee PR, Moosa MM & Deniz AA (2016) Two-dimensional crowding uncovers a hidden conformation of α-synuclein. *Angew Chemie – Int Ed* **55**, 12789–12792.
152 Liu W, Fu L, Wang Z, Sohrabpour Z, Li X, Liu Y, Wang H & Yan ECY (2018) Two dimensional crowding effects on protein folding at interfaces observed by chiral vibrational sum frequency generation spectroscopy. *Phys Chem Chem Phys* **20**, 22421–22426.
153 Ye C, Chai Q, Zhong M & Wei Y (2013) Effect of crowding by Ficolls on OmpA and OmpT refolding and membrane insertion. *Protein Sci* **22**, 239–245.
154 De Geyter J, Tsirigotaki A, Orfanoudaki G, Zorzini V, Economou A & Karamanou S (2016) Protein folding in the cell envelope of *Escherichia coli*. *Nat Microbiol* **1**, 16107.
155 McNulty BC, Young GB & Pielak GJ (2006) Macromolecular crowding in the *Escherichia coli* periplasm maintains α-synuclein disorder. *J Mol Biol* **355**, 893–897.
156 Colclasure GC & Parker JC (1991) Cytosolic protein concentration is the primary volume signal dog red cells. *J Gen Physiol* **98**, 881–892.
157 Karasawa A, Swier LJYM, Stuart MCA, Brouwers J, Helms B & Poolman B (2013) Physicochemical factors controlling the activity and energy coupling of an ionic strength-gated ATP-binding cassette (ABC) transporter. *J Biol Chem* **288**, 29862–29871.
158 Culham DE, Meinecke M & Wood JM (2012) Impacts of the osmolality and the lumenal ionic strength on osmosensory transporter ProP in proteoliposomes. *J Biol Chem* **287**, 27813–27822.
159 Ressl S, Terwisscha Van Scheltinga AC, Vonrhein C, Ott V & Ziegler C (2009) Molecular basis of transport and regulation in the Na+/betaine symporter BetP. *Nature* **458**, 47–52.
160 Rowe I, Anishkin A, Kamaraju K, Yoshimura K & Sukharev S (2014) The cytoplasmic cage domain of the mechanosensitive channel MscS is a sensor of macromolecular crowding. *J Gen Physiol* **143**, 543–557.
161 Perozo E, Kloda A, Cortes DM & Martinac B (2002) Physical principles underlying the transduction of bilayer deformation forces during mechanosensitive channel gating. *Nat Struct Biol* **9**, 696–703.
162 Lindén M, Sens P & Phillips R (2012) Entropic tension in crowded membranes. *PLoS Comput Biol* **8**, e1002431.
163 Agarraberes FA & Dice JF (2001) Protein translocation across membranes. *Biochim Biophys Acta – Biomembr* **1513**, 1–24.

164 Gopinathan A & Kim YW (2007) Polymer translocation in crowded environments. *Phys Rev Lett* **99**, 228106.
165 Cao WP, Sun LZ, Wang C & Luo MB (2011) Monte Carlo simulation on polymer translocation in crowded environment. *J Chem Phys* **135**, 174901.
166 Chen Y & Luo K (2013) Dynamics of polymer translocation through a nanopore induced by different sizes of crowding agents. *J Chem Phys* **138**, 204903.
167 Larimi MG, Mayse LA & Movileanu L (2019) Interactions of a polypeptide with a protein nanopore under crowding conditions. *ACS Nano* **13**, 4469–4477.
168 Ayub M & Bayley H (2016) Engineered transmembrane pores. *Curr Opin Chem Biol* **34**, 117–126.
169 Lipowsky R, Risselada HJ, Jahn R, Sykes C, Baumgart T, Frolov VA, Dimova R, Lauritsen L, Voth GA, Deserno M *et al.* (2018) The 2018 biomembrane curvature and remodeling roadmap. *J Phys D Appl Phys* **51**, 343001.
170 Kozlov MM, Campelo F, Liska N, Chernomordik LV, Marrink SJ & McMahon HT (2014) Mechanisms shaping cell membranes. *Curr Opin Cell Biol* **29**, 53–60.
171 Zimmerberg J & Gawrisch K (2006) The physical chemistry of biological membranes. *Nat Chem Biol* **2**, 564–567.
172 Shi Z & Baumgart T (2015) Membrane tension and peripheral protein density mediate membrane shape transitions. *Nat Commun* **6**, 5974.
173 Franquelim HG, Khmelinskaia A, Sobczak JP, Dietz H & Schwille P (2018) Membrane sculpting by curved DNA origami scaffolds. *Nat Commun* **9**, 811.
174 Snead WT, Hayden CC, Gadok AK, Zhao C, Lafer EM, Rangamani P & Stachowiak JC (2017) Membrane fission by protein crowding. *Proc Natl Acad Sci U S A*. **114**, E3258–E3267.
175 Stachowiak JC, Hayden CC & Sasaki DY (2010) Steric confinement of proteins on lipid membranes can drive curvature and tubulation. *Proc Natl Acad Sci U S A* **107**, 7781–7786.
176 Chen Z, Atefi E & Baumgart T (2016) Membrane shape instability induced by protein crowding. *Biophys J* **111**, 1823–1826.
177 Dahmani I, Ludwig K & Chiantia S (2019) Influenza A matrix protein M1 induces lipid membrane deformation via protein multimerization. *Biosci Rep* **39**, BSR20191024.
178 Steinkühler J, Knorr RL, Zhao Z, Bhatia T, Bartelt SM, Wegner S, Dimova R & Lipowsky R (2020) Controlled division of cell-sized vesicles by low densities of membrane-bound proteins. *Nat Commun* **11**, 905.
179 Van Der Lee R, Buljan M, Lang B, Weatheritt RJ, Daughdrill GW, Dunker AK, Fuxreiter M, Gough J, Gsponer J, Jones DT *et al.* (2014) Classification of intrinsically disordered regions and proteins. *Chem Rev* **114**, 6589–6631.
180 Busch DJ, Houser JR, Hayden CC, Sherman MB, Lafer EM & Stachowiak JC (2015) Intrinsically disordered proteins drive membrane curvature. *Nat Commun* **6**, 7875.
181 Snead WT, Zeno WF, Kago G, Perkins RW, Blair Richter J, Zhao C, Lafer EM & Stachowiak JC (2019) BAR scaffolds drive membrane fission by crowding disordered domains. *J Cell Biol* **218**, 664–682.
182 Siaw HMH, Raghunath G & Dyer RB (2018) Peripheral protein unfolding drives membrane bending. *Langmuir* **34**, 8400–8407.
183 Doyle DA, Cabral JM, Pfuetzner RA, Kuo A, Gulbis JM, Cohen SL, Chait BT & MacKinnon R (1998) The structure of the potassium channel: molecular basis of K+ conduction and selectivity. *Science* **280**, 69–77.
184 Fowler PW, Hélie J, Duncan A, Chavent M, Koldsø H & Sansom MSP (2016) Membrane stiffness is modified by integral membrane proteins. *Soft Matter* **12**, 7792–7803.
185 Madsen JJ, Grime JMA, Rossman JS & Voth GA (2018) Entropic forces drive clustering and spatial localization of influenza A M2 during viral budding. *Proc Natl Acad Sci U S A* **115**, E8595–E8603.
186 Paulino J, Pang X, Hung I, Zhou HX & Cross TA (2019) Influenza A M2 channel clustering at high protein/lipid ratios: viral budding implications. *Biophys J* **116**, 1075–1084.
187 Klusch N, Murphy BJ, Mills DJ, Yildiz Ö & Kühlbrandt W (2017) Structural basis of proton translocation and force generation in mitochondrial ATP synthase. *Elife* **6**, e33274.
188 Dudkina NV, Heinemeyer J, Keegstra W, Boekema EJ & Braun HP (2005) Structure of dimeric ATP synthase from mitochondria: An angular association of monomers induces the strong curvature of the inner membrane. *FEBS Lett* **579**, 5769–5772.
189 Blum TB, Hahn A, Meier T, Davies KM & Kühlbrandt W (2019) Dimers of mitochondrial ATP synthase induce membrane curvature and self-assemble into rows. *Proc Natl Acad Sci U S A* **116**, 4250–4255.
190 Scheve CS, Gonzales PA, Momin N & Stachowiak JC (2013) Steric pressure between membrane-bound proteins opposes lipid phase separation. *J Am Chem Soc* **135**, 1185–1188.
191 Zeno WF, Johnson KE, Sasaki DY, Risbud SH & Longo ML (2016) Dynamics of crowding-induced mixing in phase separated lipid bilayers. *J Phys Chem B* **120**, 11180–11190.
192 Imam ZI, Kenyon LE, Carrillo A, Espinoza I, Nagib F & Stachowiak JC (2016) Steric pressure among membrane-bound polymers opposes lipid phase separation. *Langmuir* **32**, 3774–3784.

193 Al-Habori M (2001) Macromolecular crowding and its role as intracellular signalling of cell volume regulation. *Int J Biochem Cell Biol* **33**, 844–864.
194 Aknoun S, Savatier J, Bon P, Galland F, Abdeladim L, Wattellier B & Monneret S (2015) Living cell dry mass measurement using quantitative phase imaging with quadriwave lateral shearing interferometry : an accuracy and sensitivity discussion quantitative phase imaging with quadriwave. *J Biomed Opt* **20**, 126009.
195 Kubitschek HE, Baldwin WW, Schroeter SJ & Graetzer R (1984) Independence of buoyant cell density and growth Rate in *Escherichia coli*. *J Bacteriol* **158**, 296–299.
196 Movasaghi Z, Rehman S & Rehman IU (2007) Raman spectroscopy of biological tissues. *Appl Spectrosc Rev* **42**, 493–541.
197 Luby-Phelps K, Castle PE, Taylor DL & Lanni F (1987) Hindered diffusion of inert tracer particles in the cytoplasm of mouse 3T3 cells. *Proc Natl Acad Sci U S A* **84**, 4910–4913.
198 Delarue M, Brittingham GP, Pfeffer S, Surovtsev IV, Pinglay S, Kennedy KJ, Schaffer M, Gutierrez JI, Sang D, Poterewicz G *et al.* (2018) mTORC1 controls phase separation and the biophysical properties of the cytoplasm by tuning crowding. *Cell* **174**, 338–349.
199 Mika JT, Thompson AJ, Dent MR, Brooks NJ, Michiels J, Hofkens J & Kuimova MK (2016) Measuring the viscosity of the *Escherichia coli* plasma membrane using molecular rotors. *Biophys J* **111**, 1528–1540.
200 Konopka MC, Shkel IA, Cayley S, Record MT & Weisshaar JC (2006) Crowding and confinement effects on protein diffusion in vivo. *J Bacteriol* **188**, 6115–6123.
201 Nawrocki G, Wang PH, Yu I, Sugita Y & Feig M (2017) Slow-down in diffusion in crowded protein solutions correlates with transient cluster formation. *J Phys Chem B* **121**, 11072–11084.
202 Schavemaker PE, Śmigiel WM & Poolman B (2017) Ribosome surface properties may impose limits on the nature of the cytoplasmic proteome. *Elife* **6**, e30084.
203 Guzman I, Gelman H, Tai J & Gruebele M (2014) The extracellular protein VlsE is destabilized inside cells. *J Mol Biol* **426**, 11–20.
204 Groen J, Foschepoth D, Te Brinke E, Boersma AJ, Imamura H, Rivas G, Heus HA & Huck WTS (2015) Associative interactions in crowded solutions of biopolymers counteract depletion effects. *J Am Chem Soc* **137**, 13041–13048.
205 Mu X, Choi S, Lang L, Mowray D, Dokholyan NV, Danielsson J & Oliveberg M (2017) Physicochemical code for quinary protein interactions in *Escherichia coli*. *Proc Natl Acad Sci U S A* **114**, E4556–E4563.
206 Gnutt D, Gao M, Brylski O, Heyden M & Ebbinghaus S (2015) Excluded-volume effects in living cells. *Angew Chemie – Int Ed* **54**, 2548–2551.
207 Murade CU & Shubeita GT (2019) A molecular sensor reveals differences in macromolecular crowding between the cytoplasm and nucleoplasm. *ACS Sensors* **4**, 1835–1843.
208 Boersma AJ, Zuhorn IS & Poolman B (2015) A sensor for quantification of macromolecular crowding in living cells. *Nat Methods* **12**, 227–229.
209 Liu B, Åberg C, van Eerden FJ, Marrink SJ, Poolman B & Boersma AJ (2017) Design and properties of genetically encoded probes for sensing macromolecular crowding. *Biophys J* **112**, 1929–1939.
210 Liu B, Mavrova SN, Van Den Berg J, Kristensen SK, Mantovanelli L, Veenhoff LM, Poolman B & Boersma AJ (2018) Influence of fluorescent protein maturation on FRET measurements in living cells. *ACS Sensors* **3**, 1735–1742.
211 Liu B, Hasrat Z, Poolman B & Boersma AJ (2019) Decreased effective macromolecular crowding in *Escherichia coli* adapted to hyperosmotic stress. *J Bacteriol* **209**, 1–11.
212 Mouton SN, Thaller DJ, Crane MM, Rempel IL, Kaeberlein M, Lusk CP, Boersma AJ & Veenhoff LM. A physicochemical roadmap of yeast replicative aging. submitted.
213 Gnutt D, Brylski O, Edengeiser E, Havenith M & Ebbinghaus S (2017) Imperfect crowding adaptation of mammalian cells towards osmotic stress and its modulation by osmolytes. *Mol Biosyst* **13**, 2218–2221.
214 Sukenik S, Ren P & Gruebele M (2017) Weak protein-protein interactions in live cells are quantified by cell-volume modulation. *Proc Natl Acad Sci U S A* **114**, 6776–6781.
215 Holcman D, Parutto P, Chambers JE, Fantham M, Young LJ, Marciniak SJ, Kaminski CF, Ron D & Avezov E (2018) Single particle trajectories reveal active endoplasmic reticulum luminal flow. *Nat Cell Biol* **20**, 1118–1125.
216 Asakura S & Oosawa F (1958) Interaction between particles suspended in solutions. *J Polym Sci* **XXXIII**, 183–192.
217 Marenduzzo D, Finan K & Cook PR (2006) The depletion attraction: An underappreciated force driving cellular organization. *J Cell Biol* **175**, 681–686.
218 Kang H, Pincus PA, Hyeon C & Thirumalai D (2015) Effects of macromolecular crowding on the collapse of biopolymers. *Phys Rev Lett* **114**, 068303.
219 Minton AP (2005) Models for excluded volume interaction between an unfolded protein and rigid macromolecular cosolutes: Macromolecular crowding and protein stability revisited. *Biophys J* **88**, 971–985.
220 Schwarz J, J Leopold H, Leighton R, Miller RC, Aplin CP, Boersma AJ, Heikal AA & Sheets ED

(2019) Macromolecular crowding effects on energy transfer efficiency and donor-acceptor distance of hetero-FRET sensors using time-resolved fluorescence. *Methods Appl Fluoresc* **7**, 025002.

221 Konopka MC, Sochacki KA, Bratton BP, Shkel IA, Record MT & Weisshaar JC (2009) Cytoplasmic protein mobility in osmotically stressed *Escherichia coli*. *J Bacteriol* **91**, 231–237.

222 Broecker J, Fiedler S, Gimpl K & Keller S (2014) Polar interactions trump hydrophobicity in stabilizing the self-inserting membrane protein mistic. *J Am Chem Soc* **136**, 13761–13768.

223 Park E & Rapoport TA (2012) Mechanisms of Sec61/SecY-mediated protein translocation across membranes. *Annu Rev Biophys* **41**, 21–40.

224 Nussinov R, Tsai CJ & Jang H (2018) Oncogenic ras isoforms signaling specificity at the membrane. *Cancer Res* **78**, 593–602.

225 Simons K & Gerl MJ (2010) Revitalizing membrane rafts: new tools and insights. *Nat Rev Mol Cell Biol* **11**, 688–699.

226 Dunstone MA & de Marco A (2017) Cryo-electron tomography: An ideal method to study membrane-associated proteins. *Philos Trans R Soc. B Biol Sci* **372**, 20160210.